STRUCTURAL ENGINEERING,
MECHANICS AND MATERIALS

ON THE FORMULATION OF CLOSEST-POINT PROJECTION ALGORITHMS IN ELASTOPLASTICITY.

PART I: THE VARIATIONAL STRUCTURE.

REPORT NO. UCB/SEMM-2000/01

BY F. ARMERO AND A. PÉREZ-FOGUET

JANUARY 2000

DEPARTMENT OF CIVIL AND ENVIRONMENTAL ENGINEERING
UNIVERSITY OF CALIFORNIA
BERKELEY, CALIFORNIA

On the Formulation of Closest-Point Projection Algorithms in Elastoplasticity. Part I: The Variational Structure.

by

F. Armero* & A. Pérez-Foguet†

Structural Engineering, Mechanics and Materials
Department of Civil and Environmental Engineering
University of California, Berkeley CA 94720, USA

Abstract

We present in this paper the characterization of the variational structure behind the discrete equations defining the closest-point projection approximation in elastoplasticity. Rate-independent and viscoplastic formulations are considered in the infinitesimal and the finite deformation range, the later in the context of isotropic finite strain multiplicative plasticity. Primal variational principles in terms of the stresses and stress-like hardening variables are presented first, followed by the formulation of dual principles incorporating explicitly the plastic multiplier. Augmented Lagrangian extensions are also presented allowing a complete regularization of the problem in the constrained rate-independent limit. The variational structure identified in this paper leads to the proper framework for the development of new improved numerical algorithms for the integration of the local constitutive equations of plasticity as it is undertaken in Part II of this work.

KEY WORDS: plasticity and viscoplasticity; return mapping algorithms; closest-point projection; primal and dual variational principles; augmented Lagrangian.

* Corresponding author (armero@ce.berkeley.edu).

† On leave from the Dept. Matemàtica Aplicada III, ETSECCPB, UPC, Barcelona, Spain, during the Fall semester 1999.

1. Introduction

One of the fundamental ingredients in the numerical solution of the initial boundary-value problem characterizing the deformation of solids and structures is the numerical integration of the constitutive equations of the material model. This integration is carried out locally at each quadrature point in typical finite element implementations. For the elastoplastic and viscoplastic models of interest in this work this process exhibits a clear, and desired, strain-driven structure by which the stresses and updated internal variables characterizing the inelastic response of the material are sought for a given strain increment and previous values of these internal variables. The consistent linearization of the resulting discrete equations proves to be crucial for the successful solution of the global boundary-value problem with a quadratically convergent Newton-Raphson scheme. In this context, the use of return mapping algorithms for the integration of the local plastic evolution equations has become standard nowadays.

The main component in return mapping algorithms is the enforcement of the plastic consistency condition defined by the yield function or, in the case of viscoplastic models, the approximation of the rate equation describing the evolution of the stress state with respect to this yield function. A common feature of many of the techniques proposed to date is the use of an operator split strategy in the solution of this problem. Briefly, the final stresses and updated internal variables are obtained by imposing these conditions after a trial state has detected the activation of the plastic evolution equations. Common to many approaches is the use of an elastic trial state in this process, leading then to a plastic corrector step approximating the plastic evolution equations. Of interest in this work is the consideration of the so-called closest-point projection approximation for this plastic corrector step, perhaps the most commonly used strategy in practical applications, both in the infinitesimal and finite deformation ranges. This strategy involves an implicit approximation of the governing equations, leading to a nonlinear system of algebraic equations in the stresses and updated internal variables. Details can be found in the following section, with complete accounts presented in several textbooks existing already on the subject; we refer the reader to recent examples of Simo & Hughes [1998], Simo [1998] and Han & Reddy [1999], among others.

Except for very particular cases where a closed-form solution can be found (the classical example being J_2-flow theory with linear hardening), an iterative algorithm needs to be applied for the solution of the resulting nonlinear system of algebraic equations. A typical choice is the use of a Newton scheme, a strategy that we refer in this work as the Newton closest-point projection algorithm. The asymptotic quadratic rate of convergence of this scheme when solving the local equations and the availability of its linearization in closed form, leading to the algorithmic tangent employed in the solution of the global boundary-value problem, makes this strategy very attractive. However, the well-known limited local convergence properties of Newton schemes, in the sense that actual convergence can only be assured for initial estimates (referring to the trial state in our case) close to the final solution, makes this approach difficult to motivate when considering the complex constitutive models used in many practical applications of interest. The results reported in de Souza Neto et al. [1994], Bićanić & Pearce [1996], Pérez–Foguet

ET AL. [1999] and in this work illustrate these difficulties, identifying regions of the stress space where due to the strong nonlinearity of the equations no convergence is attained in practice. A common case occurs near points of the yield surface with large curvature. It is interesting to note that this situation occurs even for associated plasticity models based on a convex yield criterion, with strain hardening and constant elasticities, that is, for cases involving completely well-posed continuum models.

Several strategies can be found in the literature to avoid these difficulties. For example, the consideration of alternative trial predictors initializing the iterative process can be found studied in DE SOUZA NETO et al. [1994], BIĆANIĆ & PEARCE [1996] and HAN & REDDY [1999]. Usually, however, these alternative definitions are specific to particular models, difficult to generalize to other more complex yield surfaces or hardening/softening laws. Iterative strategies involving line search schemes can be found also in the literature as in, e.g., DUTKO et al [1993]. Existing approaches, however, do not take into account explicitly the constrained character of the equations, as it is considered in detail in Part II of this work. Similarly, the consideration of sub-stepping techniques has been proposed to alleviate the convergence difficulties when integrating complex constitutive models; see, for example, OWEN & HINTON [1980], SLOAN [1987] and ABBO & SLOAN [1996]. Recent works along this line can be found in PÉREZ–FOGUET ET AL. [1999], where an adaptive sub-stepping technique has been proposed involving a Newton closest-point projection algorithm for each sub-step, with a complete derivation of the final algorithmic tangent resulting of the consistent linearization of this process. However, the resulting algorithmic consistent tangent is no longer symmetric, and the generalization of this sub-stepping strategy to the finite deformation case is unclear.

Alternatively, we can find in the literature other approaches than abandon altogether the original closest-point projection approximation. An early example of this type of approaches is the so-called cutting plane algorithm presented in SIMO & ORTIZ [1985] and ORTIZ & SIMO [1986], based on a steepest descent strategy avoiding an implicit treatment of the governing equations. The resulting scheme involves an explicit iterative process, thus exhibiting improved convergence properties. However, no expression exists for the algorithmic consistent linearization making the use of these techniques somehow limited in actual finite element implementations employing a Newton-Raphson solution strategy. Furthermore, these schemes show a poorer accuracy properties when compared with the original closest-point projection approximation, as reported in SIMO [1998], page 252.

Other approaches considering alternatives to the original equations of the closest-point projection approximation have appeared more recently. For example, the application of multi-step schemes (backward difference schemes, more precisely) and alternative Runge-Kutta one-step methods for the integration of the plastic evolution equations can be found in PAPADOPOULOS & TAYLOR [1994] and SIMO [1998]. These approaches usually lead, however, to even more complex implicit nonlinear system of algebraic equations, exhibiting the same difficulties in their iterative solution.

In contrast with all the aforementioned references, the work presented herein focuses on the original closest-point projection approximation and addresses the formulation of robust numerical strategies for the solution of the resulting system of equations. The

final goal of this work is the development of practical numerical algorithms for the local integration of the equations of rate-independent elastoplasticity and viscoplasticity that exhibit global convergence properties. To this purpose, it shows crucial to understand the mathematical structure behind the discrete equations defined by the closest-point projection approximation, the variational structure to be more precise, as we undertake in this first part of a series of two papers. Part II develops the actual numerical algorithms, including different representative numerical simulations in the general finite deformation range of isotropic multiplicative plasticity to illustrate their performance.

The characterization of the continuum problem of plasticity and viscoplasticity as a variational inequality can be found treated in detail in the literature for the infinitesimal case; see e.g. Duvaut & Lions [1976], Johnson [1976,78], Matthies [1979], Matthies et al [1979], Suquet [1980,81] and Anzellotti & Giaquinta [1982]. The books by Temam [1985] and, more recently, Han & Reddy [1999] present a complete and detailed account. The main purpose in these works is the characterization of the existence and regularity of the solutions of the global boundary-value problem of (visco-)elastoplasticity, with the main emphasis given to the development of the proper functional setting for the displacement and stress fields. The goal in this work is totally different. As noted above, we focus entirely on the local discrete equations of the closest-point projection approximation at a fixed point of the solid (a quadrature point), and develop new integration algorithms for the resulting local nonlinear system of algebraic equations. In this context, the new variational formulations of these local discrete equations developed in this Part I clearly identify the different strategies to follow in arriving to efficient numerical algorithms for the local integration of general (visco-)elastoplastic models, including the finite deformation range.

The complete characterization of this variational structure requires, obviously, some limiting assumptions on the underlying physical model. In this way, the assumption of associated plasticity based on a convex elastic domain with strain hardening (or perfect plasticity) is required for a rigorous characterization of this structure. Nevertheless, the numerical algorithms considered herein are formulated for the general case not fitting in this framework. We note that the analyses considered in the aforementioned more limited situations have actually motivated the formulation of the new algorithms proposed in this work, still exhibiting an improved numerical performance in more general situations not encompassed in the specific assumptions considered in this paper. Remarkably the results presented herein apply equally to such models in both the infinitesimal and the finite deformation range, the latter for the case of isotropic multiplicative plasticity, thanks to the common form of the final equations when an exponential mapping strategy is applied in their integration; see Simo [1992,99], and references therein, for details.

As implied by the name "closest-point projection", a clear variational structure exists behind this technique, namely, the minimization of the distance in the proper metric between the trial state and the admissible elastic set defined by the yield function in stress space. This result can be found discussed in detail in Simo & Hughes [1998] for the case of constant elasticities and linear strain hardening. It is the first goal of this paper to present an extension of this result to the general nonlinear case, an important extension especially

when considering general finite deformation models. In this context, we formulate a primal variational principle involving the stresses and stress-like internal variables. Motivated by the structure of this principle, a constrained variational principle in the rate-independent case, we investigate the formulation of alternative dual variational principles in the context of the classical theory of constrained optimization. The same approach is taken for the viscoplastic problem. Moreover, new augmented Lagrangian formulations are presented for the problem at hand, allowing the regularization of the original constrained equations in the rate-independent case, and thus leading to the proper framework for the formulation of new and improved numerical algorithms for their numerical integration.

We note that this rich variational structure of the problem is a reflection of a similar structure of the underlying continuum problem, namely, the classical principle of maximum plastic dissipation. A successful numerical integration of the governing equations must inherit this structure. As shown by the results in this work, the analysis of the mathematical structure behind the discrete equations allows to identify efficient numerical schemes fitting this structure of the continuum problem and exhibiting global convergence, a property not shared by the traditional Newton closest-point projection algorithm, even under the aforementioned convexity assumptions, despite the erroneous belief that can be found sometimes in the literature. We refer to Part II of this work for a complete discussion of these issues in the development of the actual numerical algorithms.

An outline of the rest of the paper is as follows. Section 2 presents a summary of the governing continuum equations and their closest-point projection approximation. Primal and dual variational formulations behind this approximation are presented and discussed in detail in Section 3 for the constrained rate-independent problem and in Section 4 for the viscoplastic problem. The aforementioned augmented Lagrangian extensions are developed in Section 5. Section 6 concludes with a brief summary and some final remarks.

2. Problem Definition

We describe in this section the equations governing the problem of interest in this work, namely, the local continuum equations of elastoplasticity and the so-called closest-point projection scheme for their numerical approximation. The developments presented in this section, although standard in the most part, clearly identify the open issues addressed in this work. We begin in Section 2.1 with the introduction of the continuum equations together with the notation employed in the rest of the paper.

2.1. The governing equations

We denote by $\boldsymbol{\varepsilon} \in \mathbb{R}^{n_\varepsilon}$ the total strain at a fixed point $\boldsymbol{X} \in \mathcal{B}$ of a solid $\mathcal{B} \subset \mathbb{R}^{n_{\rm dim}}$ ($n_{\rm dim} = 1, 2,$ or 3), in practice, a quadrature point in a typical finite element solution of the equations governing its mechanical equilibrium. All the considerations in the rest of the paper occur at this local level (at $\boldsymbol{X} \in \mathcal{B}$), so further reference to this situation is omitted hereafter. In the infinitesimal case, the strains $\boldsymbol{\varepsilon}$ are simply identified as the symmetric part

of the gradient of the displacements; the finite deformation case is considered in Section 2.3 below. In this setting, the strains $\boldsymbol{\varepsilon}$ are assumed decomposed additively as

$$\boldsymbol{\varepsilon} = \boldsymbol{\varepsilon}^e + \boldsymbol{\varepsilon}^p \ , \tag{2.1}$$

identifying the elastic strains $\boldsymbol{\varepsilon}^e \in \mathbb{R}^{n_\varepsilon}$ and the plastic strains $\boldsymbol{\varepsilon}^p \in \mathbb{R}^{n_\varepsilon}$, as it is customary in elastoplasticity. We denote by n_ε the number of strain degrees of freedom (e.g. $n_\varepsilon = 6$ in general three-dimensional problems) in the above considerations.

Let $\boldsymbol{\sigma} \in \mathbb{R}^{n_\varepsilon}$ and $\boldsymbol{q} \in \mathbb{R}^{n_\alpha}$ denote the stress and a set of n_α stress-like internal variables characterizing the hardening/softening of the material, respectively. In particular, the perfectly plastic case is recovered by considering $\boldsymbol{q} \equiv 0$ throughout. Standard thermodynamic arguments identify the constitutive relations

$$\boldsymbol{\sigma} = \partial_{\boldsymbol{\varepsilon}^e} \psi(\boldsymbol{\varepsilon}^e, \boldsymbol{\alpha}) \ , \qquad \text{and} \qquad \boldsymbol{q} = -\partial_{\boldsymbol{\alpha}} \psi(\boldsymbol{\varepsilon}^e, \boldsymbol{\alpha}) \ , \tag{2.2}$$

for the stored energy function ψ in terms of the elastic strains $\boldsymbol{\varepsilon}^e$ and a general set of strain-like variables $\boldsymbol{\alpha} \in \mathbb{R}^{n_\alpha}$ conjugate to the original variables $\boldsymbol{q}$. Uncoupled thermomechanical conditions (e.g. isothermal conditions, with ψ corresponding to the Helmholtz free energy function) are assumed in the above relations, as it is the focus in this paper. The functional form

$$\psi(\boldsymbol{\varepsilon}^e, \boldsymbol{\alpha}) = \psi^e(\boldsymbol{\varepsilon}^e) + \psi^h(\boldsymbol{\alpha}) \ , \tag{2.3}$$

for two separate potentials ψ^e and ψ^h is commonly assumed, although the particular form (2.3) is not employed in the considerations that follow.

The definition of the elastoplastic model is completed with the introduction of the evolution equations for the plastic internal variables (the plastic strains $\boldsymbol{\varepsilon}^p$ and hardening variables $\boldsymbol{\alpha}$). These evolution equations read in general form

$$\dot{\boldsymbol{\varepsilon}}^p = \gamma \, \boldsymbol{m}_\sigma(\boldsymbol{\sigma}, \boldsymbol{q}) \ , \qquad \text{and} \qquad \dot{\boldsymbol{\alpha}} = \gamma \, \boldsymbol{m}_q(\boldsymbol{\sigma}, \boldsymbol{q}) \ , \tag{2.4}$$

where the symbol $\dot{(\cdot)}$ denotes the time derivative. Here we have introduced the (scalar) plastic multiplier γ, and the general flow vectors $\boldsymbol{m}_\sigma(\boldsymbol{\sigma}, \boldsymbol{q})$ and $\boldsymbol{m}_q(\boldsymbol{\sigma}, \boldsymbol{q})$, functions of the stress $\boldsymbol{\sigma}$ and stress-like variables $\boldsymbol{q}$, that is, we consider the structure of the equations referred to as stress-based plasticity. In this context, the plastic multiplier γ is determined by the classical Kuhn-Tucker complementary conditions

$$\gamma \geq 0 \ , \quad f(\boldsymbol{\sigma}, \boldsymbol{q}) \leq 0 \ , \quad \text{and} \quad \gamma f(\boldsymbol{\sigma}, \boldsymbol{q}) = 0 \tag{2.5}$$

for the yield function $f(\boldsymbol{\sigma}, \boldsymbol{q})$, and the consistency condition

$$\gamma \dot{f}(\boldsymbol{\sigma}, \boldsymbol{q}) = 0 \ , \tag{2.6}$$

for $\gamma > 0$. Equations (2.5) characterize the loading/unloading conditions with equation (2.6) defining the persistency of the plastic state during plastic flow.

For future use in the developments that follow, we observe that the flow rule $(2.4)_1$ can be written in the equivalent form

$$\dot{\boldsymbol{\varepsilon}}^e = \dot{\boldsymbol{\varepsilon}} \, - \, \gamma \, \boldsymbol{m}_\sigma(\boldsymbol{\sigma}, \boldsymbol{q}) \, . \tag{2.7}$$

after making use of the additive decomposition (2.1). As described in the following section, the equation (2.7), together with the stress-based form of the relations (2.5) and (2.6), clearly identifies the strain driven structure of the problem. That is, given an increment of the total strain $\boldsymbol{\varepsilon}$ (or, equivalently, the strain rate $\dot{\boldsymbol{\varepsilon}}$) determine the corresponding increment in the stress $\boldsymbol{\sigma}$ and plastic internal variables $\{\boldsymbol{\varepsilon}^p, \boldsymbol{\alpha}\}$, and corresponding $\boldsymbol{q}$. In this respect, we note that the enforcement of the consistency condition (2.6) allows to arrive at the expression

$$\gamma = \frac{1}{\nabla f \cdot \tilde{\boldsymbol{G}} \, \boldsymbol{m}} \left(\partial^2_{\boldsymbol{\varepsilon}^e \boldsymbol{\varepsilon}^e} \psi \; \partial_\sigma f - \partial^2_{\boldsymbol{\varepsilon}^e \alpha} \psi \; \partial_q f \right) \cdot \dot{\boldsymbol{\varepsilon}} \, , \tag{2.8}$$

for the plastic multiplier γ after combining the governing equations (2.1) to (2.6). In (2.8), we have introduced the notation

$$\boldsymbol{m} := \left\{ \begin{array}{c} \boldsymbol{m}_\sigma \\ \boldsymbol{m}_q \end{array} \right\} \qquad \text{and} \qquad \nabla f = \left\{ \begin{array}{c} \partial_\sigma f \\ \partial_q f \end{array} \right\} \, , \tag{2.9}$$

with "$\cdot$" denoting the standard Euclidean inner product in the space with the appropriate dimension implied from the context. Similarly, denoting the Hessian of the stored energy function ψ by

$$\boldsymbol{G} := \nabla^2 \psi = \begin{pmatrix} \partial^2_{\boldsymbol{\varepsilon}^e \boldsymbol{\varepsilon}^e} \psi & \partial^2_{\boldsymbol{\varepsilon}^e \alpha} \psi \\ \partial^2_{\alpha \boldsymbol{\varepsilon}^e} \psi & \partial^2_{\alpha\alpha} \psi \end{pmatrix} \, , \tag{2.10}$$

and introducing the matrix

$$\mathbb{J} := \begin{pmatrix} \boldsymbol{I}_{n_\varepsilon} & \boldsymbol{0} \\ \boldsymbol{0} & -\boldsymbol{I}_{n_\alpha} \end{pmatrix} \, , \tag{2.11}$$

for the identity matrices $\boldsymbol{I}_{n_\varepsilon}$ and $\boldsymbol{I}_{n_\alpha}$ in $\mathbb{R}^{n_\varepsilon}$ and $\mathbb{R}^{n_\alpha}$, respectively, the (symmetric) matrix $\tilde{\boldsymbol{G}}$ in (2.8) reads

$$\tilde{\boldsymbol{G}} := \mathbb{J} \; \boldsymbol{G} \; \mathbb{J}^T = \begin{pmatrix} \partial^2_{\boldsymbol{\varepsilon}^e \boldsymbol{\varepsilon}^e} \psi & -\partial^2_{\boldsymbol{\varepsilon}^e \alpha} \psi \\ -\partial^2_{\alpha \boldsymbol{\varepsilon}^e} \psi & \partial^2_{\alpha\alpha} \psi \end{pmatrix} \, , \tag{2.12}$$

where $(\cdot)^T$ denotes the matrix transpose. We note the relations

$$\mathbb{J} = \mathbb{J}^T = \mathbb{J}^{-1} \, . \tag{2.13}$$

Given the expression (2.8), the common assumption

$$\nabla f \cdot \tilde{\boldsymbol{G}} \, \boldsymbol{m} > 0 \, , \tag{2.14}$$

is introduced, so the governing equations (2.2) to (2.6) define uniquely the plastic multiplier γ.

For future use, we note that the Hessian $\boldsymbol{G}$ in (2.10) is block-diagonal for the stored energy function ψ of the form (2.3), that is, we have in this case

$$\boldsymbol{G} = \begin{pmatrix} \mathbb{C} & 0 \\ 0 & \mathbb{D} \end{pmatrix} \tag{2.15}$$

for the elastic tangent $\mathbb{C} := \nabla^2 \psi^e(\boldsymbol{\varepsilon}^e)$ and the hardening modulus $\mathbb{D} := \nabla^2 \psi^h(\boldsymbol{\alpha})$. Note also that, $\tilde{\boldsymbol{G}} = \boldsymbol{G}$ in this case.

The alternative case of viscoplasticiy can be easily recovered from the previous expressions by replacing the relations (2.5) and (2.6) by the explicit definition

$$\gamma = \frac{1}{\eta}\, g(f)\ , \tag{2.16}$$

for a material viscosity parameter $\eta \geq 0$, and a general scalar function satisfying the conditions

$$g(f) = 0 \qquad \text{for} \quad f \leq 0\ , \qquad \text{and} \quad g'(f) > 0 \qquad \text{for} \quad f > 0\ , \tag{2.17}$$

for its first derivative $g'(\cdot)$, that is, monotonically increasing function $g(f)$ of the yield function for $f > 0$ (no longer restricted to non-positive values). This condition is shown in Section 4 to lead to the proper convexity requirements for the variational principles developed in that section. A common and simple form of the function $g(f)$ is given by

$$g(f) = \langle f \rangle = \begin{cases} f & \text{for } f \geq 0, \\ 0 & \text{for } f \leq 0, \end{cases} \tag{2.18}$$

for the Macaulay brackets $\langle \cdot \rangle$. The equation (2.16) corresponds to the so-called Perzyna regularization (see Perzyna [1966,71]), recovering the unilaterally constrained problem of rate-independent elastoplasticity in the limit $\eta \to 0$ of zero viscosity. We refer to the model defined by (2.18) as the linear viscoplastic model.

Remark 2.1. *Some remarks on notation.* The symbol $\nabla(\cdot)$ in (2.8) and thereafter denotes the gradient with respect to all the arguments of the function under consideration, with $\nabla^2(\cdot)$ corresponding to the second gradient. The gradient with respect to a particular argument of the function is denoted by $\partial(\cdot)$ with the sub-index denoting the argument, as in (2.2), and with $\partial^2(\cdot)$ denoting the second gradient with respect the specified sub-indices. Similarly, the dual role of the stresses and strains motivates the introduction below of the compact notation $\boldsymbol{\Sigma} := \{\boldsymbol{\sigma}, \boldsymbol{q}\}$ and $\mathcal{I} := \{\boldsymbol{\varepsilon}^e, -\boldsymbol{\alpha}\}$, both in $\mathbb{R}^{n_\varepsilon + n_\alpha}$. We prefer, however, to state the main results in the original notation, hence showing more directly their physical meaning as well as the actual numerical implementation of the different expressions, while using this compact notation whenever is more convenient in the algebraic manipulations. □

2.2. The closest-point projection approximation

The constitutive relations described in the previous section need to be integrated in time, usually in a strain-driven structure. In this framework, the stresses and internal variables are updated from their known values at certain time for a given strain increment in time. More precisely, we consider a typical time increment $[t_n, t_{n+1}]$, with time step $\Delta t := t_{n+1} - t_n$. All the variables are known at t_n and a strain increment $\Delta\boldsymbol{\varepsilon}_{n+1}$ is given leading to a total strain

$$\boldsymbol{\varepsilon}_{n+1} = \boldsymbol{\varepsilon}_n + \Delta\boldsymbol{\varepsilon}_{n+1} \ , \tag{2.19}$$

at t_{n+1} in the infinitesimal range considered in this section; see Section 2.3 for its counterpart in the finite deformation range. The goal is to obtain the new stresses $\boldsymbol{\sigma}_{n+1}$ and update the plastic internal variables $\{\boldsymbol{\varepsilon}^p_{n+1}, \boldsymbol{\alpha}_{n+1}\}$ (and corresponding $\boldsymbol{q}_{n+1}$) at t_{n+1}.

To this purpose, a common strategy is the use of a backward-Euler type approximation of the governing equations (2.4). The resulting discrete equations read in residual form as

$$\left.\begin{aligned} -\boldsymbol{\varepsilon}^p_{n+1} + \boldsymbol{\varepsilon}^p_n + \Delta\gamma\ \boldsymbol{m}_\sigma(\boldsymbol{\sigma}_{n+1}, \boldsymbol{q}_{n+1}) = 0 \ , \\ -\boldsymbol{\alpha}_{n+1} + \boldsymbol{\alpha}_n + \Delta\gamma\ \boldsymbol{m}_q(\boldsymbol{\sigma}_{n+1}, \boldsymbol{q}_{n+1}) = 0 \ , \end{aligned}\right\} \tag{2.20}$$

for the discrete plastic multiplier $\Delta\gamma$ $(= \gamma_{n+1}\ \Delta t)$ satisfying the loading unloading conditions

$$\Delta\gamma \geq 0 \ , \quad f_{n+1} \leq 0 \quad \text{and} \quad \Delta\gamma\ f_{n+1} = 0 \ , \tag{2.21}$$

for $f_{n+1} := f(\boldsymbol{\sigma}_{n+1}, \boldsymbol{q}_{n+1})$. Here, the stresses $\boldsymbol{\sigma}_{n+1}$ and the stress-like internal variables $\boldsymbol{q}_{n+1}$ are given by the direct evaluation of the relations (2.2), that is,

$$\left.\begin{aligned} \boldsymbol{\sigma}_{n+1} = \ \ \partial_{\varepsilon^e}\psi(\boldsymbol{\varepsilon}^e_{n+1}, \boldsymbol{\alpha}_{n+1}) \\ \boldsymbol{q}_{n+1} = -\partial_\alpha\psi(\boldsymbol{\varepsilon}^e_{n+1}, \boldsymbol{\alpha}_{n+1}) \end{aligned}\right\} \qquad \text{for} \quad \boldsymbol{\varepsilon}^e_{n+1} := \boldsymbol{\varepsilon}_{n+1} - \boldsymbol{\varepsilon}^p_{n+1} \ . \tag{2.22}$$

The equations (2.20) to (2.22) are referred generically as the closest-point projection approximation; see Simo & Hughes [1998] and the additional discussion presented in Section 3 below for a motivation on this terminology. They easily extend to the viscoplastic model defined by equation (2.16) through the replacement of the equations (2.21) by the relation

$$\Delta\gamma = \frac{1}{\widehat{\eta}}\ g(f_{n+1}) \ , \quad \text{for} \quad \widehat{\eta} := \frac{\eta}{\Delta t} \ , \tag{2.23}$$

a backward-Euler approximation of (2.16).

The numerical solution of the algebraic system of equations defined by the relations (2.20) to (2.22) is usually accomplished following a predictor/corrector strategy. A common consideration for the predictor is the introduction of the elastic trial state defined by the known values

$$\boldsymbol{\varepsilon}^{p,trial}_{n+1} := \boldsymbol{\varepsilon}^p_n \quad \text{and} \quad \boldsymbol{\alpha}^{trial}_{n+1} := \boldsymbol{\alpha}_n \ , \tag{2.24}$$

and the corresponding stress values

$$\left.\begin{array}{rl} \boldsymbol{\sigma}_{n+1}^{trial} = & \partial_{\varepsilon^e}\psi(\boldsymbol{\varepsilon}_{n+1}^{e,trial}, \boldsymbol{\alpha}_{n+1}^{trial}) \\ \boldsymbol{q}_{n+1}^{trial} = & -\partial_{\alpha}\psi(\boldsymbol{\varepsilon}_{n+1}^{e,trial}, \boldsymbol{\alpha}_{n+1}^{trial}) \end{array}\right\} \quad \text{for} \quad \boldsymbol{\varepsilon}_{n+1}^{e,trial} = \boldsymbol{\varepsilon}_{n+1} - \boldsymbol{\varepsilon}_{n}^{p} \ , \tag{2.25}$$

that is, the values given by equations (2.20) to (2.22) with $\Delta\gamma = 0$. Note that $\boldsymbol{q}_{n+1}^{trial} = \boldsymbol{q}_n$ for the usual case given by the stored energy function (2.3). In this context

$$\texttt{IF} \quad f_{n+1}^{trial} := f(\boldsymbol{\sigma}_{n+1}^{trial}, \boldsymbol{q}_{n+1}^{trial}) \leq 0 \ , \quad \texttt{THEN} \quad (\cdot)_{n+1} = (\cdot)_{n+1}^{trial} \ , \tag{2.26}$$

that is, the trial state is taken as the final solution. Otherwise, a solution with $\Delta\gamma > 0$ is sought, thus leading to a so-called plastic corrector step. The simplicity of this strategy motivates the use of the elastic predictor (2.24) in front of other choices. For future use, we note that the system of equations (2.20) can be written equivalently as

$$\boxed{\left.\begin{array}{l} \boldsymbol{\varepsilon}_{n+1}^{e} - \boldsymbol{\varepsilon}_{n+1}^{e,trial} + \Delta\gamma \ \boldsymbol{m}_{\sigma_{n+1}} = 0 \ , \\ -\boldsymbol{\alpha}_{n+1} + \boldsymbol{\alpha}_{n+1}^{trial} + \Delta\gamma \ \boldsymbol{m}_{q_{n+1}} = 0 \ , \end{array}\right\}} \tag{2.27}$$

in terms of the elastic strains $\boldsymbol{\varepsilon}_{n+1}^{e}$ and $\boldsymbol{\varepsilon}_{n+1}^{e,trial}$ given by (2.22) and (2.25), respectively.

A typical strategy for the solution of the nonlinear equations (2.20) to (2.22) in a plastic step (i.e. for $\Delta\gamma > 0$) is the use of a Newton iterative scheme. In this work, we refer to the final algorithm as *the Newton closest-point projection scheme.* It is well-known that Newton schemes converge if the initial estimate is closed enough to the final solution, exhibiting an asymptotic quadratic rate of convergence when this happens. This quadratic rate of convergence makes the algorithm very attractive from a computational point of view, but the local character of its convergence properties (in other words, the algorithm is not globally convergent) may lead to serious difficulties. For the problem of interest herein, if the elastic trial state is too far from the final solution, the algorithm has shown no convergence in practical applications involving a yield surface with a high curvature. Several examples illustrating this fact are presented in Part II of this work. It is precisely the goal of this paper to define alternative strategies for the solution of the closest-point projection equations (2.20) to (2.22). To develop these new strategies, it shows crucial to understand the variational structure behind these equations, a structure that is discussed in the following sections.

Remarks 2.2.

1. Of interest in the numerical implementation of the elastoplastic integration schemes is the availability of the so-called elastoplastic algorithmic consistent tangent, defined by the discrete linearized relation $d\boldsymbol{\sigma}_{n+1} = \mathbb{C}_{n+1}^{ep} d\boldsymbol{\varepsilon}_{n+1}$. As noted above, the new algorithms presented in this work involve an improved solution of the closest-point projection equations (2.20) to (2.22), satisfying them upon convergence. Therefore,

the elastoplastic consistent tangent $\mathbb{C}^{ep}_{n+1}$ has the same form as for the more standard Newton closest-point projection scheme, which can be found in SIMO & HUGHES [1998] (page 147), among others.

2. We also refer to this last reference for generalizations involving a generalized mid-point approximation, whereby the discrete equations (2.20) to (2.23) involve the generalized mid-point values $(\cdot)_{n+\vartheta} = \vartheta\ (\cdot)_{n+1} + (1-\vartheta)\ (\cdot)_n$ for $\vartheta \in [0,1]$ ($\vartheta = 1$ in the preceding developments). In the variational setting described in Section 3.1 below, this option corresponds to the closest-point projection at the intermediate time $t_{n+\vartheta}$, leading to the same results as developed next for the most common case of $\vartheta = 1$. Details are omitted.

3. It is well known that the predictor/corrector strategy considered above fits within the framework of fractional-step methods based on the formulation of operator splits of the governing equations; see again SIMO & HUGHES [1998] (Section 3.5, page 139). In particular, the plastic corrector can be understood as an approximation to the rate equation

$$\frac{d\boldsymbol{\Sigma}_{cont}(\bar{\gamma})}{d\bar{\gamma}} = -\tilde{\boldsymbol{G}}\ \boldsymbol{m}(\boldsymbol{\Sigma}_{cont}(\bar{\gamma})) \qquad \text{with} \quad \boldsymbol{\Sigma}_{cont}(0) = \boldsymbol{\Sigma}^{trial}_{n+1}\ , \tag{2.28}$$

for a constant strain (i.e., $\dot{\boldsymbol{\varepsilon}} = 0$), in terms of $\boldsymbol{\Sigma} := \{\boldsymbol{\sigma}, \boldsymbol{q}\}$, and $\boldsymbol{G}$ and $\boldsymbol{m}$ defined in (2.10) and $(2.9)_1$, respectively. The subscript "*cont*" has been introduced to refer to the continuum character of equation (2.28), in contrast with a discrete counterpart introduced in later sections. The discrete plastic multiplier $\Delta\gamma$ corresponds then in the inviscid case to the value of $\bar{\gamma}$ such that

$$\bar{f}_{cont}(\Delta\gamma) = 0 \qquad \text{where} \quad \bar{f}_{cont}(\bar{\gamma}) := f(\boldsymbol{\Sigma}_{cont}(\bar{\gamma}))\ . \tag{2.29}$$

for the solution curve $\boldsymbol{\Sigma}(\bar{\gamma})$ of the continuum equation (2.28). A straightforward calculation shows that

$$\frac{d\bar{f}_{cont}}{d\bar{\gamma}} = -\nabla f \cdot \tilde{\boldsymbol{G}}\ \boldsymbol{m} < 0\ , \tag{2.30}$$

by (2.14), thus showing the dissipative character of the rate equation (2.28) in terms of the function $\bar{f}_{cont}$ defined in (2.29). It is important to emphasize that this property together with the convexity of the yield surface $f(\boldsymbol{\Sigma})$ does not assure that the standard Newton closest-point projection is globally convergent, a statement to be confronted with the discussion presented in SIMO & HUGHES [1998], page 142. In fact, the convergence of the Newton closest-point projection algorithm is an open problem, as indicated in the very last sentence in HAN & REDDY [1999]. This situation is to be expected since this algorithm does not take into account the specific structure defined by equations (2.28) to (2.30). We present in Part II of this work alternative closest-point algorithms that account for the structure defined by these equations. □

2.3. The finite deformation case

Remarkably, the discrete equations described in the previous section apply both to the infinitesimal case and the case of isotropic multiplicative finite strain plasticity. This is accomplished after using the exponential mapping in the numerical approximation for the later case; see SIMO [1992,99] and references therein for complete details. Briefly, the multiplicative decomposition of the deformation gradient $\boldsymbol{F} = \boldsymbol{F}^e\boldsymbol{F}^p$ in an elastic $\boldsymbol{F}^e$ and plastic $\boldsymbol{F}^p$ parts leads in the isotropic case of plastic and elastic relations (that is, isotropic functions define the yield surface and the elastic potential) to the flow rule

$$\boldsymbol{\pounds}_v\boldsymbol{b}^e = -\tfrac{1}{2}\gamma\ \hat{\boldsymbol{m}}_\sigma\ \boldsymbol{b}^e\ , \quad \text{where} \quad \boldsymbol{\pounds}_v\boldsymbol{b}^e := \dot{\boldsymbol{b}}^e - \boldsymbol{l}\boldsymbol{b}^e - \boldsymbol{b}^e\boldsymbol{l}^T\ , \tag{2.31}$$

for the elastic left Cauchy-Green strain tensor $\boldsymbol{b}^e = \boldsymbol{F}^e\boldsymbol{F}^{e^T}$ and the rate of deformation tensor $\boldsymbol{l} = \dot{\boldsymbol{F}}\boldsymbol{F}^{-1}$. The flow vector $\hat{\boldsymbol{m}}_\sigma$ in $(2.4)_1$ is given by the normal to the yield surface $f(\hat{\boldsymbol{\sigma}}, q)$, an isotropic function of the stress tensor $\hat{\boldsymbol{\sigma}}$, in the associated case (i.e., $\hat{\boldsymbol{m}}_\sigma = \partial_\sigma f$). Note that $\hat{\boldsymbol{\sigma}}$ denotes the so-called Kirchhoff stress tensor in this finite deformation range.

The elastic trial state is obtained by considering, as in the infinitesimal case, no evolution of the plastic variables ($\gamma = 0$ in (2.31)), leading to the trial elastic left Cauchy-Green tensor

$$\boldsymbol{b}^{e,trial}_{n+1} = \boldsymbol{f}_{n+1}\boldsymbol{b}^e_n\boldsymbol{f}^T_{n+1}\ , \tag{2.32}$$

for the incremental deformation gradient $\boldsymbol{f}_{n+1} := \boldsymbol{F}_{n+1}\boldsymbol{F}_n^{-1}$, where $\boldsymbol{F}_n$ and $\boldsymbol{F}_{n+1}$ are the deformation gradients at t_n and t_{n+1}, respectively. Note that $\boldsymbol{f}_{n+1}$ is known given the strain-driven structure of the problem. The trial value (2.32) defines a frame indifferent (objective) approximation of the equation (2.31) for $\gamma = 0$, that is, of the last two terms in $(2.31)_2$.

In the operator split framework mentioned in Remark 2.2.3, the plastic corrector step requires the approximation of the plastic flow vector contribution (i.e, the equation $\dot{\boldsymbol{b}}^e = -\gamma\ \hat{\boldsymbol{m}}_\sigma\boldsymbol{b}^e/2$), an approximation that is easily achieved through the use of the exponential map. In the isotropic case of interest, the principal directions of the stress tensor $\hat{\boldsymbol{\sigma}}_{n+1}$, the flow vector $\hat{\boldsymbol{m}}_\sigma$, and the left Cauchy-Green tensors $\boldsymbol{b}^{e,trial}_{n+1}$ and $\boldsymbol{b}^e_{n+1}$ coincide. Denoting the elastic principal stretches by λ^e_A $(A = 1, 3)$, the square root of the eigenvalues of $\boldsymbol{b}^e$ at the particular configuration, and the elastic (natural) logarithmic principal strains

$$\boldsymbol{\varepsilon}^{e,trial}_{n+1} := \left\{ \begin{array}{c} \ln(\lambda^{e,trial}_{1_{n+1}}) \\ \ln(\lambda^{e,trial}_{2_{n+1}}) \\ \ln(\lambda^{e,trial}_{3_{n+1}}) \end{array} \right\}\ , \quad \text{and} \qquad \boldsymbol{\varepsilon}^e_{n+1} := \left\{ \begin{array}{c} \ln(\lambda^{e}_{1_{n+1}}) \\ \ln(\lambda^{e}_{2_{n+1}}) \\ \ln(\lambda^{e}_{3_{n+1}}) \end{array} \right\}\ , \tag{2.33}$$

the final discrete approximation of the flow rule in the plastic corrector step reads

$$\boldsymbol{\varepsilon}^e_{n+1} - \boldsymbol{\varepsilon}^{e,trial}_{n+1} + \Delta\gamma\ \boldsymbol{m}_{\sigma_{n+1}} = 0\ , \tag{2.34}$$

that is, exactly as in equation (2.27) for the infinitesimal case. Here, the flow vector $\boldsymbol{m}_\sigma$ corresponds to the principal values of the flow tensor $\hat{\boldsymbol{m}}_\sigma$ and the stresses $\boldsymbol{\sigma} = \{\sigma_1\ \sigma_2\ \sigma_3\}^T$

correspond to the principal values σ_A of the Kirchhoff stress tensor $\hat{\boldsymbol{\sigma}}$, following the notation in (2.33). Similarly, the principal values $\boldsymbol{\sigma}$ of the Kirchhoff stress and the principal values of the elastic natural strain $\boldsymbol{\varepsilon}^e = \{\epsilon_1^e \; \epsilon_2^e \; \epsilon_3^e\}^T$ are related by a potential of the form (2.2) in the assumed isotropic finite hyperelastic case. Note that $n_\varepsilon = 3$ in this setting.

The final discrete equations correspond then exactly to the closest-point projection equations described in the previous section. In particular, the same Newton closest-point projection algorithm can be employed in their solution. The analysis presented next applies then to this case. In fact, all the numerical examples reported in Part II of this paper have been obtained in this finite deformation setting.

3. The Rate-Independent Problem

Of interest in the numerical analyses presented in forthcoming sections is to identify some important mathematical properties of the closest-point projection approximation. More precisely, it proves crucial to identify the variational structure of the system of discrete equations (2.21), (2.22) and (2.27) defining the closest-point projection, thus gaining the insight needed in the development of algorithms for their numerical solution. To this purpose, we develop in this section this variational structure for the rate-independent problem in a more general context than usually found in the literature, as discussed next. The viscoplastic problem is considered separately in Section 4 below.

The existence of this variational structure relies crucially on specific forms of the general evolution equations presented in the previous section. In particular, we introduce the following two fundamental assumptions:

Assumption 1. The elastic potential $\psi(\boldsymbol{\varepsilon}^e, \boldsymbol{\alpha})$ is a strictly convex* function in both arguments $\boldsymbol{\varepsilon}^e$ and $\boldsymbol{\alpha}$. Since in the developments that follow we are more interested in the differential form of the closest-point projection, we consider whenever needed the stronger assumption of a twice differentiable elastic potential $\psi(\boldsymbol{\varepsilon}^e, \boldsymbol{\alpha})$ with a positive definite Hessian matrix $\boldsymbol{G}$ in (2.10), that is,

$$\boldsymbol{a} \cdot \boldsymbol{G}\boldsymbol{a} > 0 \qquad \forall \boldsymbol{a} \in \mathbb{R}^{n_\varepsilon + n_\alpha} - \{\boldsymbol{0}\} \; . \tag{3.1}$$

We note that (3.1) implies the original assumption of strict convexity of the elastic potential, but not viceversa.

Assumption 2. The evolution equations (2.4) are assumed to be associated for a convex yield function $f(\boldsymbol{\sigma}, \boldsymbol{q})$, that is, the normality rules

$$\boldsymbol{m}_\sigma = \partial_\sigma f \qquad \text{and} \qquad \boldsymbol{m}_q = \partial_q f \; , \tag{3.2}$$

* Remember that a function $W(\boldsymbol{x})$ is convex iff $W(\vartheta \boldsymbol{x} + (1-\vartheta)\boldsymbol{x}^*) \leq \vartheta \; W(\boldsymbol{x}) + (1 - \vartheta) \; W(\boldsymbol{x}^*)$ for $\vartheta \in [0,1]$, being strictly convex if this inequality is strict for $\vartheta \in (0,1)$.

apply for the plastic flow vectors in the case of a differentiable yield function. Furthermore, degenerate points with $\nabla f := \{\partial_\sigma f,\, \partial_q f\}^T = 0$ are excluded.

Even though the algorithms developed in Part II of this work are formulated in the general setting described in the previous section, not involving necessarily the above assumptions, we need the variational structure to prove rigorously some of the theoretical results presented in sections to follow, thus restricting these proofs to these assumptions. The need of these assumptions is to be expected, since otherwise the well-posedness of the global initial-value boundary problem (in the classical sense that a unique solution exists depending continuously on the data) does not necessarily hold. We refer to Duvaut & Lions [1976], among others, for complete details on this regard.

A careful look of Assumption 1 for the common case given by a stored energy function of the form (2.3) reveals that this assumption implies the positive definiteness of the elastic tangent $\mathbb{C}$ and the hardening modulus $\mathbb{D}$. The positive definiteness of the elastic tangent $\mathbb{C}$ is a common and realistic assumption, even in the general finite deformation case discussed in Section 2.3. Note that this tangent is defined in terms of the principal strain measures (2.33), corresponding to the natural logarithmic strains. The assumption of positive definiteness of $\mathbb{D}$ eliminates problems involving strain softening. We note that the associated perfectly plastic limit is covered by Assumption 1 since, as noted above, the internal variables $\boldsymbol{\alpha}$ and $\boldsymbol{q}$ are not even considered in this case to begin with.

Remark 3.1. The assumed differentiability of the elastic potential ψ and the yield function f in Assumptions 1 and 2, respectively, has been introduced for simplicity in the presentation. The more general case of yield criteria with corners, for example, can be treated in the context of non-smooth convex analysis (see e.g. Ekeland & Temam [1976]), leading to the general multi-surface treatment of the plastic evolution equations, an approach that goes back to Koiter [1960] (see e.g. Simo & Hughes [1998], Chapter 5). The examples presented in Part II of this work do involve yield functions with continuous first derivatives, so details are omitted in this respect. □

3.1. A primal variational formulation

We first introduce the complementary energy function through the classical Legendre transform

$$\begin{aligned}\chi(\boldsymbol{\sigma},\boldsymbol{q}) :&= \max_{\{\boldsymbol{\varepsilon}^e,\boldsymbol{\alpha}\}} \{\boldsymbol{\sigma}\cdot\boldsymbol{\varepsilon}^e - \boldsymbol{q}\cdot\boldsymbol{\alpha} - \psi(\boldsymbol{\varepsilon}^e,\boldsymbol{\alpha})\} \\ &= \boldsymbol{\sigma}\cdot\widehat{\boldsymbol{\varepsilon}}^e(\boldsymbol{\sigma},\boldsymbol{q}) - \boldsymbol{q}\cdot\widehat{\boldsymbol{\alpha}}(\boldsymbol{\sigma},\boldsymbol{q}) - \psi(\widehat{\boldsymbol{\varepsilon}}^e(\boldsymbol{\sigma},\boldsymbol{q}),\widehat{\boldsymbol{\alpha}}(\boldsymbol{\sigma},\boldsymbol{q}))\,, \end{aligned} \tag{3.3}$$

for $\widehat{\boldsymbol{\varepsilon}}^e(\boldsymbol{\sigma},\boldsymbol{q})$ and $\widehat{\boldsymbol{\alpha}}(\boldsymbol{\sigma},\boldsymbol{q})$ being the inverse relations of (2.2). Note that these relations are invertible, so (3.3) is well-defined, under the convexity Assumption 1. In fact, the inverse relations can be written as

$$\boldsymbol{\varepsilon}^e = \partial_\sigma\chi(\boldsymbol{\sigma},\boldsymbol{q})\,, \qquad \text{and} \qquad \boldsymbol{\alpha} = -\partial_q\chi(\boldsymbol{\sigma},\boldsymbol{q})\,, \tag{3.4}$$

as a simple calculation based on the chain rule shows. A classical result in convex analysis shows the convexity of the complementary energy χ from the convexity of the stored energy function ψ. As a matter of fact, we can easily obtain the result

$$\nabla^2 \chi = \tilde{\boldsymbol{G}}^{-1} \, , \tag{3.5}$$

for $\tilde{\boldsymbol{G}}$ defined in (2.12). One easily concludes from the expression (2.12) with (2.13) that the positive definiteness condition (3.1) implies that $\tilde{\boldsymbol{G}}$ is also positive definite, thus implying the convexity of the complementary energy χ. Clearly, the complementary energy $\chi(\boldsymbol{\sigma}, \boldsymbol{q})$ has the uncoupled form

$$\chi(\boldsymbol{\sigma}, \boldsymbol{q}) = \chi^e(\boldsymbol{\sigma}) + \chi^h(\boldsymbol{q}) \, , \tag{3.6}$$

when the stored energy function ψ has the form (2.3), with χ^e and χ^h being the Legendre transforms of ψ^e and ψ^h, respectively.

With these definitions at hand, the main result in this section can be summarized with the following proposition:

Proposition 3.1 *(A primal variational principle) Under Assumptions 1 and 2, the discrete equations (2.27) defining with (2.21) and (2.22) the closest-point projection approximation can be obtained as the first-order necessary conditions of the unilaterally constrained variational problem*

$$\min_{\substack{\{\boldsymbol{\sigma}, \boldsymbol{q}\} \\ f(\boldsymbol{\sigma}, \boldsymbol{q}) \leq 0}} \left\{ \chi(\boldsymbol{\sigma}, \boldsymbol{q}) - \boldsymbol{\varepsilon}_{n+1}^{e,trial} \cdot \boldsymbol{\sigma} + \boldsymbol{\alpha}_{n+1}^{trial} \cdot \boldsymbol{q} \right\} , \tag{3.7}$$

for $\boldsymbol{\varepsilon}^{e,trial}$ and $\boldsymbol{\alpha}_{n+1}^{trial}$ defined by $(2.25)_2$ and $(2.24)_2$, respectively. Furthermore, the solution of (3.7), if it exists, is unique and gives the unique solution of the closest-point projection equations.

Proof: Following standard arguments in constrained optimization, we introduce the Lagrangian associated to the variational problem (3.7), namely,

$$\mathcal{L}(\boldsymbol{\sigma}, \boldsymbol{q}, \bar{\gamma}) := \chi(\boldsymbol{\sigma}, \boldsymbol{q}) - \boldsymbol{\varepsilon}_{n+1}^{e,trial} \cdot \boldsymbol{\sigma} + \boldsymbol{\alpha}_{n+1}^{trial} \cdot \boldsymbol{q} + \bar{\gamma} \; f(\boldsymbol{\sigma}, \boldsymbol{q}) \, , \tag{3.8}$$

for the Lagrange multiplier field $\bar{\gamma}$. Given the assumed differentiability stated in Assumptions 1 and 2, the first order necessary conditions for the local minima of the unilaterally constrained problem (3.7) (denoted by $\{\boldsymbol{\sigma}_{n+1}, \boldsymbol{q}_{n+1}\}$ with a Lagrange multiplier $\Delta\gamma$, in what follows) read

$$\partial_\sigma \mathcal{L}\Big|_{\{\boldsymbol{\sigma}_{n+1}, \boldsymbol{q}_{n+1}, \Delta\gamma\}} = \underbrace{\partial_\sigma \chi(\boldsymbol{\sigma}_{n+1}, \boldsymbol{q}_{n+1})}_{= \boldsymbol{\varepsilon}_{n+1}^e \text{ by } (3.4)_1} - \boldsymbol{\varepsilon}_{n+1}^{e,trial} + \Delta\gamma \; \partial_\sigma f(\boldsymbol{\sigma}_{n+1}, \boldsymbol{q}_{n+1}) = 0 \, , \tag{3.9}$$

$$\partial_q \mathcal{L}\Big|_{\{\boldsymbol{\sigma}_{n+1}, \boldsymbol{q}_{n+1}, \Delta\gamma\}} = \underbrace{\partial_q \chi(\boldsymbol{\sigma}_{n+1}, \boldsymbol{q}_{n+1})}_{= -\boldsymbol{\alpha}_{n+1} \text{ by } (3.4)_2} + \boldsymbol{\alpha}_{n+1}^{trial} + \Delta\gamma \; \partial_q f(\boldsymbol{\sigma}_{n+1}, \boldsymbol{q}_{n+1}) = 0 \, , \tag{3.10}$$

together with the complimentary conditions

$$\Delta\gamma \geq 0 \ , \quad f_{n+1} := f(\boldsymbol{\sigma}_{n+1}, \boldsymbol{q}_{n+1}) \leq 0 \quad \text{and} \quad \Delta\gamma f_{n+1} = 0 \ . \tag{3.11}$$

Equations (3.9), (3.10) and (3.11) correspond exactly to $(2.27)_1$, $(2.27)_2$ and (2.21), thus proving the first part of the proposition.

The above results use the differentiability conditions incorporated in Assumptions 1 and 2, but do not use explicitly the assumed convexity. This assumption is used in concluding the equivalence between the global minimizer of (3.7) and the solution of the Euler-Lagrange equations (3.9) and (3.10), including their uniqueness (see e.g. EKELAND & TEMAM [1976], page 35). Briefly, the (strict) convexity of the complementary energy leads to the (strict) convexity of the function being minimized in (3.7), since the linear terms in $\{\boldsymbol{\sigma}, \boldsymbol{q}\}$ do not affect this property. We note in this respect the positive definiteness of the Hessian of the Lagrangian (3.8)

$$\partial^2_{\sigma q}\mathcal{L} = \nabla^2\chi + \bar{\gamma}\ \nabla^2 f \ , \tag{3.12}$$

in the $\{\boldsymbol{\sigma}, \boldsymbol{q}\}$ arguments for $\bar{\gamma} \geq 0$ under these assumptions. The resulting convexity implies that any solution of the Euler-Lagrange equations (3.9)-(3.10) is also a global minimizer in (3.7). The uniqueness follows from the strict convexity of this function. □

It is instructive to particularize the preceding developments to the case of a constant Hessian $\tilde{\boldsymbol{G}}$ of the uncoupled form (2.15), that is, for the quadratic potentials

$$\psi(\boldsymbol{\varepsilon}^e, \boldsymbol{\alpha}) = \tfrac{1}{2}\boldsymbol{\varepsilon}^e \cdot \mathbb{C}\boldsymbol{\varepsilon}^e + \tfrac{1}{2}\ \boldsymbol{\alpha} \cdot \mathbb{D}\boldsymbol{\alpha} \quad \Longleftrightarrow \quad \chi(\boldsymbol{\sigma}, \boldsymbol{q}) = \tfrac{1}{2}\boldsymbol{\sigma} \cdot \mathbb{C}^{-1}\boldsymbol{\sigma} + \tfrac{1}{2}\boldsymbol{q} \cdot \mathbb{D}^{-1}\boldsymbol{q} \ . \tag{3.13}$$

In this case, the variational problem (3.7) reads

$$\begin{aligned} \min_{\substack{\{\boldsymbol{\sigma}, \boldsymbol{q}\} \\ f(\boldsymbol{\sigma}, \boldsymbol{q}) \leq 0}} \quad & \Big\{ \tfrac{1}{2}(\boldsymbol{\sigma} - \boldsymbol{\sigma}^{trial}_{n+1}) \cdot \mathbb{C}^{-1}(\boldsymbol{\sigma} - \boldsymbol{\sigma}^{trial}_{n+1}) \\ & + \tfrac{1}{2}(\boldsymbol{q} - \boldsymbol{q}^{trial}_{n+1}) \cdot \mathbb{D}^{-1}(\boldsymbol{q} - \boldsymbol{q}^{trial}_{n+1}) - \chi(\boldsymbol{\sigma}^{trial}_{n+1}, \boldsymbol{q}^{trial}_{n+1}) \Big\} \ , \end{aligned} \tag{3.14}$$

for the constant trial values $\{\boldsymbol{\sigma}^{trial}_{n+1}, \boldsymbol{q}^{trial}_{n+1}\}$ defined in (2.25). Up to the constant value $\chi(\boldsymbol{\sigma}^{trial}_{n+1}, \boldsymbol{q}^{trial}_{n+1})$, the variational problem (3.14) is precisely the expression of the variational formulation found in the literature for this case of quadratic potentials; see SIMO & HUGHES [1998] (page 119). Observe that the shift by this constant does not affect the final outcome of the variational problem; alternatively, we could have added the constant value $\chi_{n+1}(\boldsymbol{\sigma}^{trial}_{n+1}, \boldsymbol{q}^{trial}_{n+1})$ to the original problem (3.7). Therefore, we conclude that the result summarized in Proposition 3.1 generalizes these existing results. Note that, as described in Section 2.3, these developments apply entirely to the case of isotropic multiplicative finite strain plasticity, where the elastic laws may be given in terms of a general hyperelastic potential, not necessarily quadratic.

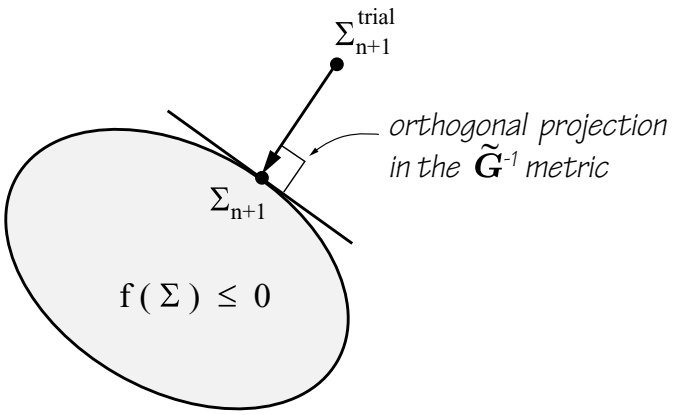

FIGURE 3.1. Sketch of the closes-point projection for quadratic potentials (constant $\tilde{\boldsymbol{G}}$). The trial state $\boldsymbol{\Sigma}_{n+1}^{trial}$ is projected onto the elastic domain $f(\boldsymbol{\Sigma}) \leq 0$, orthogonality in the metric $\tilde{\boldsymbol{G}}^{-1}$, leading to the solution $\boldsymbol{\Sigma}_{n+1}$.

The geometric interpretation of the variational problem (3.7) becomes clear after (3.14), namely the minimization of the distance between the trial state and the elastic domain defined by the yield condition $(2.21)_2$ in the norm induced by $\tilde{\boldsymbol{G}}^{-1}$, thus the common name of closest-point projection. Figure 3.1, found in the aforementioned reference, sketches this idea. The solution $\boldsymbol{\Sigma}_{n+1} = \{\boldsymbol{\sigma}_{n+1}, \boldsymbol{q}_{n+1}\}$ can be seen to correspond to the projection of the trial value $\boldsymbol{\Sigma}_{n+1}^{trial} = \{\boldsymbol{\sigma}_{n+1}^{trial}, \boldsymbol{q}_{n+1}^{trial}\}$ onto the elastic domain $f(\boldsymbol{\Sigma}) \leq 0$, the projection being orthogonal in the $\tilde{\boldsymbol{G}}^{-1}$ metric.

Proposition 3.1 addresses the uniqueness of the solution of the problem of interest under the considered assumptions, but not its existence. Assuming that $\chi(\tilde{\boldsymbol{\Sigma}}) < +\infty$ for some $\tilde{\boldsymbol{\Sigma}} \in \mathbb{E}$, where $\mathbb{E}$ denotes the (assumed convex) elastic domain

$$\mathbb{E} := \{\boldsymbol{\Sigma} \mid f(\boldsymbol{\Sigma}) \leq 0\} \subset \mathbb{R}^{n_\varepsilon + n_\alpha} \tag{3.15}$$

(a trivial assumption in the case of interest herein), then the existence of a solution of the minimization problem (3.7) follows trivially if $\mathbb{E}$ is bounded. Otherwise, the existence of a solution follows if the function being minimized, that is,

$$\Pi(\boldsymbol{\Sigma}) := \chi(\boldsymbol{\Sigma}) - \mathcal{I}^{trial} \cdot \boldsymbol{\Sigma} \,, \tag{3.16}$$

where $\mathcal{I}^{trial} := \{\boldsymbol{\varepsilon}_{n+1}^{e,trial}, -\boldsymbol{\alpha}_{n+1}^{trial}\}$ in the compact notation introduced in Remark 2.1, satisfies the growth condition

$$\Pi(\boldsymbol{\Sigma}) \to \infty \quad \text{for} \quad \|\boldsymbol{\Sigma}\| \to \infty \,, \tag{3.17}$$

in $\mathbb{E}$, where we have considered the Euclidean norm $\|\boldsymbol{\Sigma}\|^2 = \boldsymbol{\Sigma} \cdot \boldsymbol{\Sigma}$ in $\mathbb{R}^{n_\varepsilon + n_\alpha}$. See e.g. Ekeland & Temam [1976] (page 35) for a proof of this classical result in convex analysis.

The growth condition (3.17) holds, for example, if the coerciveness condition

$$\chi(\boldsymbol{\Sigma}) \geq C_1 \|\boldsymbol{\Sigma}\|^p + C_2 \quad \text{for} \quad p > 1 \,, \tag{3.18}$$

and constants $C_1 > 0$ and C_2, is required for the complementary energy function χ. This is the case because the last term in (3.16), the linear term in $\boldsymbol{\Sigma}$, does not affect the coerciveness condition (3.18) for the function $\mathit{\Pi}(\cdot)$, since $p > 1$. The coerciveness condition (3.18) is not a restrictive assumption, even in the finite deformation case considered in Section 2.3. In fact, a common example conforming with this assumption is provided by a quadratic potential (i.e. $\chi(\boldsymbol{\Sigma}) = \boldsymbol{\Sigma} \cdot \tilde{\boldsymbol{G}}^{-1} \boldsymbol{\Sigma}/2$), as in the particular example in (3.13). This case corresponds to the classical law of linear elasticity in the infinitesimal range or the so-called Hencky's laws of finite elasticity in the finite deformation range (note that $\boldsymbol{\varepsilon}^e$ stands for the (elastic) natural logarithmic strain), both in combination with linear hardening. In these cases, condition (3.18) holds with $p = 2$ given the continuity and strict convexity conditions in Assumption 1, resulting respectively in a bounded and invertible Hessian $\tilde{\boldsymbol{G}}$.

The variational problem (3.7) corresponds to the primal variational formulation for the unilaterally constrained problem of interest. Here, we are referring to the local constitutive problem and primal in the classical sense of constrained optimization theory, not to be confused with the terminology used when considering the global initial-boundary value problem. In this context, the variational problem defined in terms of the displacement and strains is usually referred to as the primal form, whereas the form in stresses and stress-like internal variables is referred as dual; see e.g Duvaut & Lions [1976] or Han & Reddy [1999], among others. Crucial to the development of the new numerical algorithms developed in Part II of this work is the use of dual forms of the variational problem (3.7). We undertake this task in the following section.

3.2. Dual variational formulations

The dual form of the variational problem (3.7) can be constructed with the definition of the dual function

$$\boxed{\begin{aligned} \phi(\bar{\gamma}) :&= \min_{\{\boldsymbol{\sigma},\boldsymbol{q}\}} \mathcal{L}(\boldsymbol{\sigma}, \boldsymbol{q}, \bar{\gamma}) \\ &= \min_{\{\boldsymbol{\sigma},\boldsymbol{q}\}} \left\{ \chi(\boldsymbol{\sigma}, \boldsymbol{q}) - \boldsymbol{\varepsilon}^{e,trial}_{n+1} \cdot \boldsymbol{\sigma} + \boldsymbol{\alpha}^{trial}_{n+1} \cdot \boldsymbol{q} + \bar{\gamma}\ f(\boldsymbol{\sigma}, \boldsymbol{q}) \right\} , \end{aligned}} \tag{3.19}$$

for $\bar{\gamma} \geq 0$. This function is well-defined given the convexity of the Lagrangian $\mathcal{L}(\boldsymbol{\sigma}, \boldsymbol{q}, \bar{\gamma})$ in the $\{\boldsymbol{\sigma}, \boldsymbol{q}\}$ components, as implied by (3.12). Remarkably the minimization problem in $\{\boldsymbol{\sigma}, \boldsymbol{q}\}$ of equation (3.19) is not constrained: the value of $\bar{\gamma}$ is fixed in this problem. Given the assumed convexity of the problem, standard results in optimization theory lead to the alternative variational formulation summarized in the following proposition.

Proposition 3.2 *(A dual variational principle) Under the Assumptions 1 and 2, the plastic multiplier $\Delta\gamma$ in the closest-point projection approximation defined by the equations (2.27) with (2.21) and (2.22) can be characterized as the argument of the variational problem*

$$\max_{\bar{\gamma}\geq 0} \phi(\bar{\gamma}) \ , \tag{3.20}$$

for the dual function $\phi(\bar{\gamma})$ defined in (3.19), and with the other components of the solution $\{\boldsymbol{\sigma}_{n+1}, \boldsymbol{q}_{n+1}\}$ given by the arguments of the unconstrained minimization problem (3.19) defining the function $\phi(\bar{\gamma})$ for $\bar{\gamma} = \Delta\gamma$.

PROOF: Apply the classical duality theorem (see e.g. LUENBERGER [1989], pages 399 to 401). □

It is of the main interest to relate the previous developments with the a-priori estimate presented in Remark 2.2.2. To this purpose, we note that the dual function (3.19) can be written equivalently as

$$\phi(\bar{\gamma}) = \chi(\boldsymbol{\sigma}(\bar{\gamma}), \boldsymbol{q}(\bar{\gamma})) - \boldsymbol{\varepsilon}^{e,trial}_{n+1} \cdot \boldsymbol{\sigma}(\bar{\gamma}) + \boldsymbol{\alpha}^{trial}_{n+1} \cdot \boldsymbol{q}(\bar{\gamma}) + \bar{\gamma}\ f(\boldsymbol{\sigma}(\bar{\gamma}), \boldsymbol{q}(\bar{\gamma})) \ , \tag{3.21}$$

where $\boldsymbol{\Sigma}(\bar{\gamma}) := \{\boldsymbol{\sigma}(\bar{\gamma}), \boldsymbol{q}(\bar{\gamma})\}$ is the solution of the equation

$$\nabla\chi(\boldsymbol{\Sigma}(\bar{\gamma})) - \mathcal{I}^{trial}_{n+1} + \bar{\gamma}\ \nabla f(\boldsymbol{\Sigma}(\bar{\gamma})) = 0 \ , \tag{3.22}$$

for $\mathcal{I}^{trial} := \{\boldsymbol{\varepsilon}^{e,trial}_{n+1}, -\boldsymbol{\alpha}^{trial}_{n+1}\}$ and for a fixed $\bar{\gamma} \geq 0$ as implied by the minimization problem in (3.19). We can already observe the connection of (3.22) with the continuum relation (2.28). Indeed, after noting that

$$\frac{d}{d\bar{\gamma}}\Big[\nabla\chi(\tilde{\boldsymbol{\Sigma}}(\bar{\gamma}))\Big] = \tilde{\boldsymbol{G}}^{-1}\ \frac{d}{d\bar{\gamma}}\Big[\tilde{\boldsymbol{\Sigma}}(\bar{\gamma})\Big] \quad \text{for any curve} \quad \tilde{\boldsymbol{\Sigma}}(\bar{\gamma}) \ , \tag{3.23}$$

we can write the continuum rate equation (2.28)

$$\left.\begin{aligned} &\frac{d}{d\bar{\gamma}}\Big[\nabla\chi(\boldsymbol{\Sigma}_{cont}(\bar{\gamma}))\Big] = -\nabla f(\boldsymbol{\Sigma}_{cont}(\bar{\gamma})) \ , \\ &\nabla\chi(\boldsymbol{\Sigma}_{cont}(0)) = \mathcal{I}^{trial}_{n+1} \ , \end{aligned}\right\} \tag{3.24}$$

for the associated case of interest in this section (so $\boldsymbol{m} = \nabla f$). The discrete expression (3.22) can be seen to be a consistent approximation of (3.24).

Observe that (3.22) defines a unique curve $\boldsymbol{\Sigma}(\bar{\gamma})$ for $\bar{\gamma} \geq 0$, the unique global minimum defined by the minimization problem in (3.19) since the function being minimized is strictly convex for $\bar{\gamma} \geq 0$. Furthermore, taking the derivative of (3.22) with respect to $\bar{\gamma}$, we obtain

$$\begin{aligned} \frac{d}{d\bar{\gamma}}\Big[\nabla\chi(\boldsymbol{\Sigma}(\bar{\gamma}))\Big] &= -\nabla f - \bar{\gamma}\ \nabla^2 f\ \frac{d\boldsymbol{\Sigma}(\bar{\gamma})}{d\bar{\gamma}} \\ &= -\nabla f - \bar{\gamma}\ \nabla^2 f\ \tilde{\boldsymbol{G}}\frac{d}{d\bar{\gamma}}\Big[\nabla\chi(\boldsymbol{\Sigma}(\bar{\gamma}))\Big] \ , \end{aligned} \tag{3.25}$$

after using (3.23). We conclude that

$$\frac{d}{d\bar{\gamma}}\Big[\nabla\chi(\boldsymbol{\Sigma}(\bar{\gamma}))\Big] = \tilde{\boldsymbol{G}}^{-1}\left[\tilde{\boldsymbol{G}}^{-1} + \bar{\gamma}\ \nabla^2 f\right]^{-1}\nabla f\ , \tag{3.26}$$

after noting that the inverses in this expression exist, since $\tilde{\boldsymbol{G}}$ and $\nabla^2 f$ are positive definite and semi-definite, respectively, by the assumed convexity and $\bar{\gamma} \geq 0$.

With the equations (3.21) and (3.22) at hand, we can compute the derivative of the dual function $\phi(\bar{\gamma})$ as

$$\frac{d\phi}{d\bar{\gamma}}(\bar{\gamma}) = \Big[\underbrace{\nabla\chi(\boldsymbol{\Sigma}(\bar{\gamma})) - \mathcal{I}_{n+1}^{trial} + \bar{\gamma}\ \nabla f(\boldsymbol{\Sigma}(\bar{\gamma}))}_{=\,0 \text{ by } (3.22)}\Big] \cdot \frac{d}{d\bar{\gamma}}\Big[\boldsymbol{\Sigma}(\bar{\gamma})\Big] + f(\boldsymbol{\Sigma}(\bar{\gamma}))\ . \tag{3.27}$$

We conclude that

$$\frac{d\phi}{d\bar{\gamma}}(\bar{\gamma}) = \bar{f}(\bar{\gamma}) \quad \text{for} \quad \bar{f}(\bar{\gamma}) = f(\boldsymbol{\Sigma}(\bar{\gamma}))\ , \tag{3.28}$$

and $\boldsymbol{\Sigma}(\bar{\gamma})$ being again the solution of the equation (3.22). Note that

$$\bar{f}(0) = f(\boldsymbol{\Sigma}_{n+1}^{trial}) = f_{n+1}^{trial}\ , \tag{3.29}$$

since, as noted above, the solution $\boldsymbol{\Sigma}(\bar{\gamma})$ of (3.22) is unique. It is apparent that the function $\bar{f}(\bar{\gamma})$ corresponds to the function $\bar{f}_{cont}(\bar{\gamma})$ in (2.29) for the continuum case.

The necessary first order condition for the maximum problem in (3.20) can then be written as

$$\frac{d\phi}{d\bar{\gamma}}(\Delta\gamma) = \bar{f}(\Delta\gamma) = 0 \qquad \text{at the maximum with} \quad \Delta\gamma > 0\ , \tag{3.30}$$

that is, the plastic consistency condition, and

$$\frac{d\phi}{d\bar{\gamma}}(0) = \bar{f}(0) \leq 0 \qquad \text{at the maximum with} \quad \Delta\gamma = 0\ . \tag{3.31}$$

In fact, given the convexity assumptions, we can easily show that $\Delta\gamma$ with $\boldsymbol{\Sigma}(\Delta\gamma)$ does satisfy the sufficient condition for a maximum of the dual function $\phi(\bar{\gamma})$ at $\bar{\gamma} = \Delta\gamma$. Indeed, we can write

$$\begin{aligned}
\frac{d^2\phi}{d\bar{\gamma}^2}(\bar{\gamma}) = \frac{d\bar{f}}{d\bar{\gamma}}(\bar{\gamma}) &= \nabla f \cdot \frac{d}{d\bar{\gamma}}\Big[\boldsymbol{\Sigma}(\bar{\gamma})\Big] \\
&= \nabla f \cdot \tilde{\boldsymbol{G}}\frac{d}{d\bar{\gamma}}\Big[\nabla\chi(\boldsymbol{\Sigma}(\bar{\gamma}))\Big] \qquad \text{by (3.23)} \\
&= -\nabla f \cdot \Big[\tilde{\boldsymbol{G}}^{-1} + \bar{\gamma}\ \nabla^2 f\Big]^{-1}\nabla f \qquad \text{by (3.26)}\ .
\end{aligned} \tag{3.32}$$

Since the matrix in this expression is positive definite, we conclude that

$$\frac{d^2\phi}{d\bar{\gamma}^2}(\bar{\gamma}) = \frac{d\bar{f}}{d\bar{\gamma}}(\bar{\gamma}) < 0 \qquad \forall \bar{\gamma} \geq 0 \,, \tag{3.33}$$

($\nabla f \neq 0$ by Assumption 2). In other words, the dual function $\phi(\bar{\gamma})$ is strictly concave, and the function $\bar{f}(\bar{\gamma})$ is monotonically decreasing for $\bar{\gamma} \geq 0$. Figure 4.2 depicts the function $\bar{f}(\bar{\gamma})$ for an elastic ($\Delta\gamma = 0$) and plastic ($\Delta\gamma > 0$ steps, including the viscoplastic case considered in the Section 4 below. The strictly concave character of the dual function concluded from (3.33) identifies $\Delta\gamma$ as the unique global maximum of $\phi(\bar{\gamma})$ in $\bar{\gamma} \in [0, \infty)$. Therefore, the characterization (3.30) and (3.31) of the maximum of (3.20) is completely equivalent to the original variational formulation itself. Proposition 3.2 can then be written equivalently as follows.

Proposition 3.3 *(An alternative dual variational principle) Under Assumptions 1 to 2, the plastic multiplier $\Delta\gamma$ in the closest-point projection approximation defined by the equations (2.27) with (2.21) and (2.22) can be characterized as the unique non-negative root of the equation*

$$\bar{f}(\Delta\gamma) = 0 \,, \quad \textit{if} \quad \bar{f}(0) = f_{n+1}^{trial} > 0 \quad (\Rightarrow \ \Delta\gamma > 0) \,, \tag{3.34}$$

or simply

$$\Delta\gamma = 0 \,, \qquad \textit{if} \quad \bar{f}(0) = f_{n+1}^{trial} \leq 0 \,, \tag{3.35}$$

for the function $\bar{f}(\bar{\gamma}) = f(\boldsymbol{\sigma}(\bar{\gamma}), \boldsymbol{q}(\bar{\gamma}))$, with $\{\boldsymbol{\sigma}(\bar{\gamma}), \boldsymbol{q}(\bar{\gamma})\}$ for $\bar{\gamma} \geq 0$ corresponding to the argument of the unconstrained minimization problem

$$\min_{\{\boldsymbol{\sigma}, \boldsymbol{q}\}} \left\{ \chi(\boldsymbol{\sigma}, \boldsymbol{q}) - \boldsymbol{\varepsilon}_{n+1}^{e,trial} \cdot \boldsymbol{\sigma} + \boldsymbol{\alpha}_{n+1}^{trial} \cdot \boldsymbol{q} + \bar{\gamma} \ f(\boldsymbol{\sigma}, \boldsymbol{q}) \right\} , \tag{3.36}$$

The other components of the solution are then simply obtained as $\{\boldsymbol{\sigma}_{n+1}, \boldsymbol{q}_{n+1}\} = \{\boldsymbol{\sigma}(\Delta\gamma), \boldsymbol{q}(\Delta\gamma)\}$.

Remarks 3.2.

1. We note that the function $\bar{f}_{cont}(\bar{\gamma})$ in (2.29) for the continuum problem (2.28) is convex under Assumptions 1 and 2 and for a constant tangent $\tilde{\boldsymbol{G}}$. Indeed, we easily obtain for this case the relation

$$\frac{d^2\,\bar{f}_{cont}(\bar{\gamma})}{d\bar{\gamma}^2} = 2 \left(\tilde{\boldsymbol{G}} \ \nabla f \right) \cdot \nabla^2 f \left(\tilde{\boldsymbol{G}} \ \nabla f \right) \geq 0 \,, \tag{3.37}$$

   illustrating the convexity of the function $\bar{f}_{cont}(\bar{\gamma})$ for the assumed convexity of the yield function f and the positive definite character of $\tilde{\boldsymbol{G}}$. This result, however, does

not apply necessarily to the general case of the same continuum problem with non-constant tangents, nor for the function $\bar{f}(\bar{\gamma})$ considered in this section, the discrete counterpart of $\bar{f}_{cont}(\bar{\gamma})$.

2. All the developments in this section considered explicitly the variational structure gained by the Assumptions 1 to 2. However, the final treatment of the governing equations does apply to the general case considered in Section 2.1, not necessarily convex or associated, as it is employed in the formulation of general solution algorithms presented in Part II of this work. In this general case, and following Proposition 3.3, the problem corresponding to a plastic step (i.e., $f_{n+1}^{trial} > 0$) can be characterized as finding the positive roots of the function $\bar{f}(\bar{\gamma})$, where $\bar{f}(\bar{\gamma}) = f(\boldsymbol{\sigma}(\bar{\gamma}), \boldsymbol{q}(\bar{\gamma}))$ for the solution $\{\boldsymbol{\sigma}(\bar{\gamma}), \boldsymbol{q}(\bar{\gamma})\}$ of the equations

$$\left.\begin{aligned} \hat{\boldsymbol{\varepsilon}}^e(\boldsymbol{\sigma}(\bar{\gamma}), \boldsymbol{q}(\bar{\gamma})) - \boldsymbol{\varepsilon}_{n+1}^{e,trial} + \bar{\gamma}\ \boldsymbol{m}_\sigma(\boldsymbol{\sigma}(\bar{\gamma}), \boldsymbol{q}(\bar{\gamma})) = 0\ , \\ -\hat{\boldsymbol{\alpha}}(\boldsymbol{\sigma}(\bar{\gamma}), \boldsymbol{q}(\bar{\gamma})) + \boldsymbol{\alpha}_{n+1}^{trial} + \bar{\gamma}\ \boldsymbol{m}_q(\boldsymbol{\sigma}(\bar{\gamma}), \boldsymbol{q}(\bar{\gamma})) = 0\ , \end{aligned}\right\} \tag{3.38}$$

for a fixed $\bar{\gamma}$, and with the elastic relations $\hat{\boldsymbol{\varepsilon}}^e(\boldsymbol{\sigma}, \boldsymbol{q})$ and $\hat{\boldsymbol{\alpha}}(\boldsymbol{\sigma}, \boldsymbol{q})$. The final solution is again obtained as $\{\boldsymbol{\sigma}_{n+1},\, \boldsymbol{q}_{n+1}\} = \{\boldsymbol{\sigma}(\Delta\gamma),\, \boldsymbol{q}(\Delta\gamma)\}$. □

4. The Viscoplastic Problem

The variational formulations developed in the previous section extend to the viscoplastic problem defined by equations (2.22), (2.27) and the viscoplastic rate equation (2.23) through the usual interpretation of these equations as the penalty regularization of the original constrained rate-independent equations; see Perzyna [1966,71] and Simo & Hughes [1998] for details. As occurred with the variational formulations presented in Section 3, the developments presented in this section lead to alternative statements of the problem in the most general case, including general non-constant elastic stress-strain relations (2.2) and general viscoplastic functions in (2.23). In this general context, we develop in Section 4.1 a primal variational formulation, with a dual formulation developed in Section 4.2.

4.1. A primal variational formulation

Given the general viscoplastic function $g(f)$ in (2.17), we introduce the function

$$h(x) = \int_{-\infty}^{x} g(\xi)\ d\xi = \begin{cases} 0 & \text{for } x \leq 0\ , \\ \displaystyle\int_0^x g(\xi)\ d\xi & \text{for } x \geq 0\ . \end{cases} \tag{4.1}$$

Given the properties (2.17), we conclude that

$$h(x) > 0\ , \quad h'(x) = g(x) > 0 \quad \text{and} \quad h''(x) = g'(x) > 0 \quad \text{for} \quad x > 0\ , \tag{4.2}$$

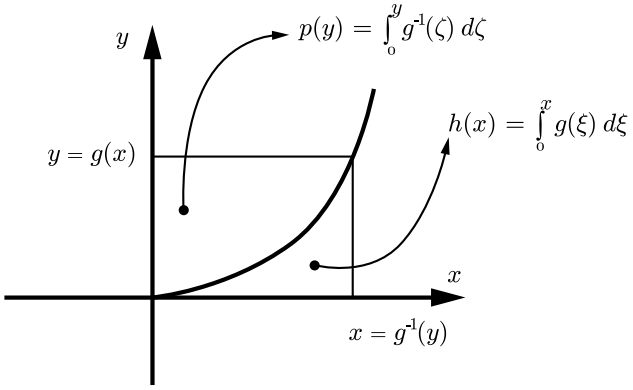

FIGURE 4.1. Definition of the different functions in the Perzyna viscoplastic regularization.

for the first and second derivatives, respectively, thus showing the convexity of the function $h(x)$ in (4.1) (strictly convex for $x > 0$). With the definition (4.2) at hand, the main result in this section can be summarized in the following proposition.

Proposition 4.1 *(A primal viscoplastic principle) Under the Assumptions 1 and 2, the discrete equations (2.27) defining with (2.22) and (2.23) the closest-point projection approximation for the viscoplastic problem can be obtained from the variational problem*

$$\min_{\{\boldsymbol{\sigma},\boldsymbol{q}\}} \left\{ \chi(\boldsymbol{\sigma},\boldsymbol{q}) - \boldsymbol{\varepsilon}_{n+1}^{e,trial} \cdot \boldsymbol{\sigma} + \boldsymbol{\alpha}_{n+1}^{trial} \cdot \boldsymbol{q} + \frac{1}{\widehat{\eta}} h\Big(f(\boldsymbol{\sigma},\boldsymbol{q}) \Big) \right\} , \tag{4.3}$$

for $\boldsymbol{\varepsilon}^{e,trial}$ and $\boldsymbol{\alpha}_{n+1}^{trial}$ defined by $(2.25)_2$ and $(2.24)_2$, respectively. Furthermore, the solution of (4.3), if it exists, is unique and gives the unique solution of the closest-point projection equations.

The proof of this proposition follows easily considering the first derivatives of the function being minimized in (4.3) and equating them to zero as necessary conditions for the minimum. Note that the variational problem (4.3) is unconstrained, with a smooth function being minimized. The strict convexity of this function (observe the positive definiteness of the corresponding Hessian given, in particular, the properties of the viscoplastic function in (4.2)) leads to the uniqueness of the solution, showing also the identity between its global minimum and the solution of the corresponding Euler-Lagrange equations, as occurred in rate-independent case summarized in Proposition 3.1. The existence of a solution follows also after imposing the growth condition (3.17) which is again implied, for example, by the coerciveness condition (3.18).

Clearly, the unconstrained variational problem (4.3) corresponds to the penalized version of the constrained problem (3.7), obtaining this in the limit $\widehat{\eta} \to 0$. In particular, no reference to the plastic multipliers $\bar{\gamma}$ is needed. These multipliers are defined a posteriori by the relation (2.16). We develop in the following section a dual variational formulation incorporating these fields explicitly

4.2. A dual variational formulation

Since the viscoplastic function $g(\cdot)$ satisfies the monotonicity condition (2.17), we can define its inverse function, denoted by $\bar{g}^{\,1}$, in the sense that

$$g(\bar{g}^{\,1}(y)) = y \qquad \text{for} \quad y \geq 0 \,. \tag{4.4}$$

Clearly, we have

$$\frac{d\bar{g}^{\,1}}{dy}(y) = \frac{1}{g'(\bar{g}^{\,1}(y))} \quad \text{for} \quad y > 0 \,, \tag{4.5}$$

where we note that $g' > 0$ for $x = \bar{g}^{\,1}(y) > 0$ (or, equivalently, $y > 0$) by (2.17). Similarly, we define the function

$$p(y) := \int_0^y \bar{g}^{\,1}(\zeta)\; d\zeta \qquad \text{so} \quad \frac{dp}{d\bar{\gamma}}(y) = \bar{g}^{\,1}(y) \qquad \text{for} \quad y \geq 0 \,. \tag{4.6}$$

We can easily see that $\bar{g}^{\,1}(0) = 0$ and $p(0) = 0$, and that

$$h(x) + p(y) = xy \,, \tag{4.7}$$

for $y = g(x)$. In fact, the function $p(y)$ corresponds to the Legendre transform of the original function $h(x)$, that is,

$$p(y) = \max_{x \geq 0} \{xy - h(x)\} \qquad \text{for} \quad y \geq 0 \,, \tag{4.8}$$

as a simple calculation shows. We also observe that

$$\bar{g}^{\,1}(y) = y \qquad \text{and} \qquad p(y) = \tfrac{1}{2}\; y^2 \qquad (y \geq 0) \,, \tag{4.9}$$

for the linear viscoplastic case defined by (2.18). These different functions are depicted in Figure 4.1.

With this notation at hand, we can write

$$\bar{\gamma} = \frac{1}{\widehat{\eta}} g(f) \quad \Longleftrightarrow \quad f = \bar{g}^{\,1}(\widehat{\eta}\;\bar{\gamma}) \quad \text{for} \quad \bar{\gamma} \geq 0 \,, \tag{4.10}$$

where the discrete viscosity parameter $\widehat{\eta} > 0$ has been defined in $(2.23)_2$ in terms of the time-step size Δt. Furthermore using (4.7), the original functional in (4.3) reads

$$\boxed{\mathcal{L}^p_{\widehat{\eta}}(\boldsymbol{\sigma}, \boldsymbol{q}, \bar{\gamma}) := \chi(\boldsymbol{\sigma}, \boldsymbol{q}) - \boldsymbol{\varepsilon}^{e,trial}_{n+1} \cdot \boldsymbol{\sigma} + \boldsymbol{\alpha}^{trial}_{n+1} \cdot \boldsymbol{q} + \bar{\gamma}\; f(\boldsymbol{\sigma}, \boldsymbol{q}) - \frac{1}{\widehat{\eta}}\; p(\widehat{\eta}\;\bar{\gamma}) \,.} \tag{4.11}$$

We refer to $\mathcal{L}^p_{\widehat{\eta}}$ as the perturbed Lagrangian for the viscoplastic problem. For the linear viscoplastic model (2.18) the last term in (4.11), the penalty term, reads simply

$$\frac{1}{\widehat{\eta}}\; p(\widehat{\eta}\;\bar{\gamma}) = \tfrac{1}{2}\;\widehat{\eta}\;\bar{\gamma}^2 \,, \tag{4.12}$$

for the viscosity parameter $\widehat{\eta} > 0$ defined in $(2.23)_2$.

We also introduce the perturbed dual function

$$\boxed{\phi^p_{\widehat{\eta}}(\bar{\gamma}) := \min_{\{\boldsymbol{\sigma},\boldsymbol{q}\}} \mathcal{L}^p_{\widehat{\eta}}(\boldsymbol{\sigma},\boldsymbol{q},\bar{\gamma}) \ ,} \tag{4.13}$$

for a fixed multiplier $\bar{\gamma} \geq 0$. This function can also be written as

$$\phi^p_{\widehat{\eta}}(\bar{\gamma}) = \chi(\boldsymbol{\Sigma}(\bar{\gamma})) - \mathcal{I}^{trial}_{n+1} \cdot \boldsymbol{\Sigma}(\bar{\gamma}) + \bar{\gamma} \ f(\boldsymbol{\Sigma}(\bar{\gamma})) - \frac{1}{\widehat{\eta}} \ p(\widehat{\eta} \ \bar{\gamma}) \ , \tag{4.14}$$

for $\mathcal{I}^{trial}_{n+1} := \{\boldsymbol{\varepsilon}^{e,trial}_{n+1}, -\boldsymbol{\alpha}^{trial}_{n+1}\}$ and $\boldsymbol{\Sigma}(\bar{\gamma}) = \{\boldsymbol{\sigma}(\bar{\gamma}), \boldsymbol{q}(\bar{\gamma})\}$ solution of the equation

$$\partial_\Sigma \mathcal{L}^p_{\widehat{\eta}} = \nabla\chi(\boldsymbol{\Sigma}(\bar{\gamma})) - \mathcal{I}^{trial}_{n+1} + \bar{\gamma} \ \nabla f(\boldsymbol{\Sigma}(\bar{\gamma})) = 0 \tag{4.15}$$

corresponding to the minimum problem in (4.13) for a fixed $\bar{\gamma} \geq 0$. Noting that

$$\partial^2_\Sigma \mathcal{L}^p_{\widehat{\eta}} = \nabla^2\chi + \bar{\gamma} \ \nabla^2 f \ , \tag{4.16}$$

is positive definite for $\bar{\gamma} \geq 0$ under Assumptions 1 and 2, that is, $\mathcal{L}^p_{\widehat{\eta}}(\cdot,\bar{\gamma})$ is strictly convex for a fixed $\bar{\gamma} \geq 0$, the solution $\boldsymbol{\Sigma}(\bar{\gamma})$ of (4.15) exists and is unique. In fact, we observe that equation (4.15) is the same as equation (3.22) for the rate-independent problem, so (3.26) also holds, and we have the very same function $\bar{f}(\bar{\gamma}) = f(\boldsymbol{\Sigma}(\bar{\gamma}))$ in $(3.28)_2$, as employed below.

With these results at hand, we can show the following proposition, the analog of Proposition 3.2 for the rate-independent problem.

Proposition 4.2 *(A dual viscoplastic variational principle) Under the Assumptions 1 and 2, the plastic multiplier $\Delta\gamma$ in the closest-point projection approximation defined by the equations (2.27) with (2.22) and (2.23) for the viscoplastic problem can be characterized as the argument of the variational problem*

$$\max_{\bar{\gamma}\geq 0} \phi^p_{\widehat{\eta}}(\bar{\gamma}) \ , \tag{4.17}$$

for the perturbed dual function $\phi^p_{\widehat{\eta}}(\bar{\gamma})$ defined by (4.13), and with the other components of the solution $\{\boldsymbol{\sigma}_{n+1}, \boldsymbol{q}_{n+1}\}$ given by the arguments of the unconstrained minimization problem (4.13) defining the function $\phi(\bar{\gamma})$ for $\bar{\gamma} = \Delta\gamma$.

PROOF: The first derivative of the perturbed dual function $\phi^p_{\widehat{\eta}}$ is given by

$$\frac{d\phi^p_{\widehat{\eta}}}{d\bar{\gamma}}(\bar{\gamma}) = \Big[\underbrace{\nabla\chi(\boldsymbol{\Sigma}(\bar{\gamma})) - \mathcal{I}^{trial}_{n+1} + \bar{\gamma} \ \nabla f(\boldsymbol{\Sigma}(\bar{\gamma}))}_{= \, 0 \text{ by } (4.15)} \Big] \cdot \frac{d}{d\bar{\gamma}} \Big[\boldsymbol{\Sigma}(\bar{\gamma}) \Big] + f(\boldsymbol{\Sigma}(\bar{\gamma})) - \frac{1}{\widehat{\eta}} \ \frac{dp}{d\bar{\gamma}}(\widehat{\eta} \ \bar{\gamma})$$

$$= f(\boldsymbol{\Sigma}(\bar{\gamma})) - \bar{g}^{\,1}(\widehat{\eta} \ \bar{\gamma}) = \bar{f}(\bar{\gamma}) - \bar{g}^{\,1}(\widehat{\eta} \ \bar{\gamma}) \ , \tag{4.18}$$

for $\bar{\gamma} \geq 0$ and the same function $\bar{f}(\bar{\gamma})$ in $(3.28)_2$. We also note that

$$\frac{d\phi^p_{\widehat{\eta}}}{d\bar{\gamma}}(0) = f(\boldsymbol{\Sigma}(0)) = f^{trial}_{n+1} \, . \tag{4.19}$$

Furthermore, the second derivative reads for $\bar{\gamma} \geq 0$

$$\begin{aligned} \frac{d^2\phi^p_{\widehat{\eta}}}{d\bar{\gamma}^2}(\bar{\gamma}) &= \nabla f \cdot \frac{d}{d\bar{\gamma}}\Big[\boldsymbol{\Sigma}(\bar{\gamma})\Big] - \frac{dp}{d\bar{\gamma}}(\bar{\gamma}) \\ &= -\nabla f \cdot \Big[\tilde{\boldsymbol{G}}^{-1} + \bar{\gamma}\ \nabla^2 f\Big]^{-1} \nabla f - \frac{\widehat{\eta}}{g'} < 0 \end{aligned} \tag{4.20}$$

after combining (3.25) and (3.26) with (4.5), and noting the positive definiteness of the matrix appearing in this expression and the condition $g' > 0$ in (2.17).

Given the expression (4.20), we conclude that the perturbed dual function $\phi^p_{\widehat{\eta}}$ is concave. Therefore, the first order necessary condition for a local maximum $\Delta\gamma$ of $\phi^p_{\widehat{\eta}}$ reads

$$\frac{d\phi^p_{\widehat{\eta}}}{d\bar{\gamma}}(\Delta\gamma) = \bar{f}(\Delta\gamma) - \bar{g}^{\,1}(\widehat{\eta}\ \Delta\gamma) = 0 \qquad \Longleftrightarrow \qquad \Delta\gamma = \frac{1}{\widehat{\eta}}\ g(\bar{f}(\Delta\gamma)) \, , \tag{4.21}$$

given the definition (4.10) of the inverse function $\bar{g}^{\,1}(\cdot)$, and

$$\Delta\gamma = 0 \qquad \text{if} \quad \frac{d\phi^p_{\widehat{\eta}}}{d\bar{\gamma}}(0) = f^{trial}_{n+1} \leq 0 \, , \tag{4.22}$$

for an elastic step. Equations (4.21) and (4.22) together with (4.15) are the original equations of the closest-point projection approximation for the viscoplastic problem, thus proving the proposition. □

Figure 4.2 sketches the relations (4.21) and (4.22) for the case of a plastic and elastic step, respectively. The solution $\Delta\gamma$ is obtained as the intersection of the curves $\bar{f}(\bar{\gamma})$ and $\widehat{\eta}\ \bar{g}^{\,1}(\bar{\gamma})$, recovering the inviscid case in the limit $\widehat{\eta} = 0$ (that is, the relations (3.34) and (3.35)). As a consequence of these considerations, we can characterize the solution of the closest-point projection approximation for the viscoplastic problem in the following equivalent form, the analog of Proposition 3.3 for the rate-independent problem.

Proposition 4.3 *(An alternative dual viscoplastic variational principle) Under Assumptions 1 and 2, the plastic multiplier $\Delta\gamma$ in the closest-point projection approximation defined by the equations (2.27) with (2.22) and (2.23) for the viscoplastic problem can be characterized as the unique non-negative root of the equation*

$$g(\bar{f}(\Delta\gamma)) - \widehat{\eta}\Delta\gamma = 0 \, , \quad \textit{if} \quad \bar{f}(0) = f^{trial}_{n+1} > 0 \quad (\Rightarrow\ \Delta\gamma > 0) \, , \tag{4.23}$$

or simply

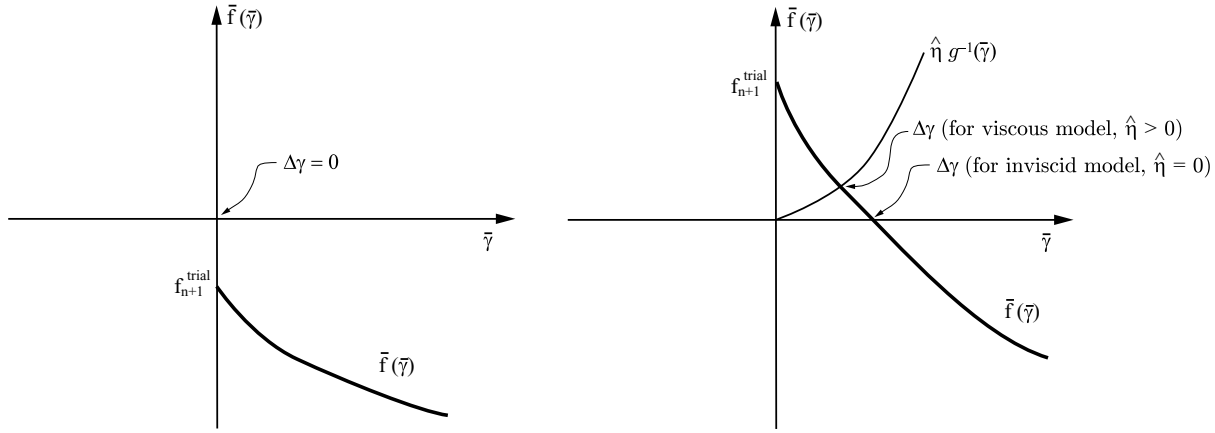

$f_{n+1}^{trial} \le 0 \;\Rightarrow\; \Delta\gamma = 0$ elastic step

$f_{n+1}^{trial} > 0 \;\Rightarrow\; \Delta\gamma > 0$ plastic step

FIGURE 4.2. Sketch of the function $\bar{f}(\bar{\gamma})$ for an elastic and plastic step in the general viscoplastic case for a viscosity parameter $\widehat{\eta}$ and viscosity function $g(\cdot)$. Note that $\bar{f}(\bar{\gamma})$ is defined for $\bar{\gamma} \geq 0$ and is monotonically decreasing, and that the curve $\widehat{\eta}\; \bar{g}^{\,1}(\bar{\gamma})$ reduces to the straight line $\widehat{\eta}\; \bar{\gamma}$ in the case of a linear viscoplastic relation.

$$\Delta\gamma = 0\,, \qquad \textit{if} \quad \bar{f}(0) = f_{n+1}^{trial} \leq 0\,, \tag{4.24}$$

for the function $\bar{f}(\bar{\gamma}) = f(\boldsymbol{\sigma}(\bar{\gamma}), \boldsymbol{q}(\bar{\gamma}))$*, with* $\{\boldsymbol{\sigma}(\bar{\gamma}), \boldsymbol{q}(\bar{\gamma})\}$ *for* $\bar{\gamma} \geq 0$ *corresponding to the argument of the unconstrained minimization problem*

$$\min_{\{\boldsymbol{\sigma},\boldsymbol{q}\}} \Big\{ \chi(\boldsymbol{\sigma}, \boldsymbol{q}) - \boldsymbol{\varepsilon}_{n+1}^{e,trial} \cdot \boldsymbol{\sigma} + \boldsymbol{\alpha}_{n+1}^{trial} \cdot \boldsymbol{q} + \bar{\gamma}\; f(\boldsymbol{\sigma}, \boldsymbol{q}) \Big\} \tag{4.25}$$

exactly as in the rate-independent problem. The other components of the solution are then simply obtained as $\{\boldsymbol{\sigma}_{n+1},\, \boldsymbol{q}_{n+1}\} = \{\boldsymbol{\sigma}(\Delta\gamma),\, \boldsymbol{q}(\Delta\gamma)\}$.

Remark 4.1. As occurred in the rate-independent limit and discussed in Remark 3.2.2, the above treatment of the governing equations applies to the general case presented in Section 2.1, not necessarily considering the convexity and associativity Assumptions 1 and 2. In this context, the solution for a visco-plastic step can be characterized as the positive roots $\Delta\gamma$ of the same equation $(4.23)_1$, with the functions $\{\boldsymbol{\sigma}(\bar{\gamma}), \boldsymbol{q}(\bar{\gamma})\}$ defining the function $\bar{f}(\bar{\gamma})$ being determined again by the solution of the general set of equations (3.38), exactly the same as in the rate-independent case. □

5. Augmented Lagrangian Extensions

The previous variational formulations form the basis for the development of the numerical algorithms presented in Part II of this work. In particular, the primal and dual principles developed in Section 3 for the rate-independent problem lead to a complete characterization behind the imposition of the consistency condition during the plastic corrector step for this case. The inclusion of additional terms penalizing the lack of satisfaction of this consistency constraint, while vanishing at the solution, leads to more general algorithms, that allows an improved numerical performance, as illustrated in the examples presented in Part II of this work. To this purpose, we develop in Sections 5.1 and 5.2 augmented extensions of the primal and dual variational formulations developed in the Section 3 for the rate-independent problem ($\eta = 0$). The viscoplastic case ($\eta > 0$) is considered as a particular case in Remark 5.2.2 in the end of Section 5.2.

5.1. The augmented Lagrangian

Following classical results of constrained optimization theory (see e.g. LUENBERGER [1989] or BERTSEKAS [1982] for complete general accounts), we consider the augmented Lagrangian associated to the unilaterally constrained primal variational problem (3.7) given by

$$\boxed{\mathcal{L}_c(\boldsymbol{\sigma}, \boldsymbol{q}, \bar{\lambda}) = \chi(\boldsymbol{\sigma}, \boldsymbol{q}) - \boldsymbol{\varepsilon}_{n+1}^{e,trial} \cdot \boldsymbol{\sigma} + \boldsymbol{\alpha}_{n+1}^{trial} \cdot \boldsymbol{q} + \frac{c}{2} \left[\langle \, \frac{\bar{\lambda}}{c} + f(\boldsymbol{\sigma}, \boldsymbol{q}) \, \rangle^2 - \left(\frac{\bar{\lambda}}{c} \right)^2 \right] ,} \tag{5.1}$$

for a constant parameter $c > 0$, the Macaulay brackets $\langle \cdot \rangle$ defined in (2.18) and a general scalar variable $\bar{\lambda}$, not constrained to be non-negative as it was the case for the plastic multiplier $\bar{\gamma} \geq 0$ employed in the previous sections. This different notation has been introduced to emphasize the unconstrained character of $\bar{\lambda}$. The final value $\Delta\gamma$ of the plastic multiplier is characterized below as a function of this newly introduced scalar variable $\bar{\lambda}$. The expression (5.1) reduces for $\bar{\lambda} + c \; f \geq 0$ to

$$\mathcal{L}_c(\boldsymbol{\sigma}, \boldsymbol{q}, \bar{\lambda}) = \mathcal{L}(\boldsymbol{\sigma}, \boldsymbol{q}, \bar{\lambda}) + \tfrac{1}{2} \; c \; [f(\boldsymbol{\sigma}, \boldsymbol{q})]^2 \, , \tag{5.2}$$

in terms of the original Lagrangian $\mathcal{L}$ in (3.8), as it is commonly found in the literature. The last term in this expression can be identified with the penalty term, as in the viscoplastic variational principle (4.3) with the linear viscoplastic model and viscosity (penalty) parameter $\widehat{\eta} = 1/c$. See Remark 5.2.2 below for an extension accommodating general (penalty) viscoplastic functions.

Setting the gradient of the augmented Lagrangian (5.1) to zero and denoting the final solution by $\{\boldsymbol{\sigma}_{n+1}, \boldsymbol{q}_{n+1}, \Delta\lambda\}$ leads to

$$\begin{aligned} \partial_\sigma \mathcal{L}_c \Big|_{\{\boldsymbol{\sigma}_{n+1}, \boldsymbol{q}_{n+1}, \Delta\lambda\}} = & \underbrace{\partial_\sigma \chi(\boldsymbol{\sigma}_{n+1}, \boldsymbol{q}_{n+1})}_{= \boldsymbol{\varepsilon}_{n+1}^e \text{ by } (3.4)_1} - \boldsymbol{\varepsilon}_{n+1}^{e,trial} \\ & + \langle \, \Delta\lambda + c \; f(\boldsymbol{\sigma}_{n+1}, \boldsymbol{q}_{n+1}) \, \rangle \; \partial_\sigma f(\boldsymbol{\sigma}_{n+1}, \boldsymbol{q}_{n+1}) = 0 \end{aligned} \tag{5.3}$$

$$\partial_q \mathcal{L}_c\Big|_{\{\boldsymbol{\sigma}_{n+1},\boldsymbol{q}_{n+1},\Delta\lambda\}} = \underbrace{\partial_q \chi(\boldsymbol{\sigma}_{n+1},\boldsymbol{q}_{n+1})}_{=\,-\boldsymbol{\alpha}_{n+1}\ \text{by}\ (3.4)_2} + \boldsymbol{\alpha}^{trial}_{n+1} + \langle\ \Delta\lambda + c\ f(\boldsymbol{\sigma}_{n+1},\boldsymbol{q}_{n+1})\ \rangle\ \partial_q f(\boldsymbol{\sigma}_{n+1},\boldsymbol{q}_{n+1}) = 0 \tag{5.4}$$

$$\partial_{\bar\lambda} \mathcal{L}_c\Big|_{\{\boldsymbol{\sigma}_{n+1},\boldsymbol{q}_{n+1},\Delta\lambda\}} = \frac{1}{c}\Big[\langle\ \Delta\lambda + c\ f(\boldsymbol{\sigma}_{n+1},\boldsymbol{q}_{n+1})\ \rangle - \Delta\lambda\Big] = 0 \tag{5.5}$$

where we have denoted the solution by $\{\boldsymbol{\sigma}_{n+1},\boldsymbol{q}_{n+1},\Delta\lambda\}$, since it indeed coincides with the solution of the original closest-point projection equations (2.27) for the assumed case of associated plasticity. In this respect, we identify the relation

$$\Delta\gamma = \langle\ \Delta\lambda + c\ f(\boldsymbol{\sigma}_{n+1},\boldsymbol{q}_{n+1})\ \rangle\ , \tag{5.6}$$

so $\Delta\gamma = 0$ if $\Delta\lambda/c + f(\boldsymbol{\sigma}_{n+1},\boldsymbol{q}_{n+1}) \le 0$ and $\Delta\gamma > 0$ otherwise. Note that, as occurred with the pairs $\bar\gamma$ and $\Delta\gamma$ employed in the previous sections, we denote by $\bar\lambda$ the general variable, with $\Delta\lambda$ corresponding to the final solution of (5.5), with no implication of any increment in the notation.

The fact that the values $\{\boldsymbol{\sigma}_{n+1},\boldsymbol{q}_{n+1},\Delta\lambda\}$ obtained as the solution of the system of equations (5.3)-(5.5) correspond with $\Delta\gamma$ given by (5.6) to the solution of the closest-point projection equations (2.27), with (2.21) and (2.22), follows after noting that

$$\begin{aligned} \Delta\lambda + c\ f_{n+1} \le 0 \quad &\Longrightarrow \quad \Delta\lambda = 0 \quad (\text{so} \quad f_{n+1} \le 0) \quad \text{by (5.5)} \\ &\Longrightarrow \quad \Delta\gamma = 0 \qquad\qquad\qquad\quad \text{by (5.6)}\ , \end{aligned} \tag{5.7}$$

and

$$\begin{aligned} \Delta\lambda + c\ f_{n+1} > 0 \quad &\Longrightarrow \quad f_{n+1} = 0 \quad (\text{so} \quad \Delta\lambda > 0) \quad \text{by (5.5)} \\ &\Longrightarrow \quad \Delta\gamma = \langle\ \Delta\lambda\ \rangle > 0 \qquad\quad \text{by (5.6)}\ , \end{aligned} \tag{5.8}$$

thus recovering the discrete Kuhn-Tucker conditions (2.21) characteristic of the rate-independent problem of interest. The combination of the two cases (5.7) and (5.8) with the equations (5.3) to (5.5) leads to the original system of equations (2.27), with (2.21) and (2.22). In particular, we identify the combination (5.8) with the plastic corrector, the case of interest in actual computations. We summarize these results in the following proposition, the augmented counterpart of Proposition 3.1.

Proposition 5.1 *(An augmented Lagrangian principle) Under the Assumptions 1 and 2, the discrete equations (2.27) defining with (2.21) and (2.22) the closest-point projection approximation for the rate-independent problem can be obtained from the variational problem*

$$\min_{\{\boldsymbol{\sigma},\boldsymbol{q}\}} \max_{\bar\lambda}\ \mathcal{L}_c(\boldsymbol{\sigma},\boldsymbol{q},\bar\lambda)\ , \tag{5.9}$$

for $c > 0$. The solution $\{\boldsymbol{\sigma}_{n+1},\boldsymbol{q}_{n+1}\}$ is obtained as the arguments of the solution of (5.9), with the plastic multiplier $\Delta\gamma$ obtained as $\Delta\gamma = \langle\ \Delta\lambda\ \rangle \ge 0$ for the last argument $\Delta\lambda$ of the solution of the problem (5.9).

The maximum character in the component $\bar{\lambda}$ is discussed in the following section when constructing the dual formulation associated to the min-max problem (5.9). Even though the consideration of the augmented Lagrangian (5.1) leads then to the same solution as the original closest-point projection equations, we observe that the equations (5.3)-(5.5) that need to be solved are different. First, note that the variational problem (5.9) is unconstrained. Second, the associated Hessian reads

$$\partial^2_{\sigma q}\mathcal{L}_c = \nabla^2\chi + \langle\ \bar{\lambda} + c\ f\ \rangle\ \nabla^2 f + H(\bar{\lambda} + c\ f)\ \nabla f \otimes \nabla f\ , \tag{5.10}$$

where $H(x) := \langle x\rangle/x \geq 0$, the Heaviside jump function, if the linear viscoplastic model is employed in the penalty regularization of the augmented Lagrangian). The convexification given by the last term in (5.10) leads to improved solution methods like, for example, Newton schemes with an enlarged region of convergence. We refer the reader to the numerical results presented in Part II of this work for an illustration of this property.

Remarks 5.1.

1. The above augmented treatment of the governing equations applies to the general case presented in Section 2.1, without reference to the variational structure implied by the Assumptions 1 and 2. In this setting, the final equations can be characterized alternatively by the augmented equations

$$\left.\begin{aligned} \hat{\boldsymbol{\varepsilon}}^e(\boldsymbol{\sigma}_{n+1},\boldsymbol{q}_{n+1}) - \boldsymbol{\varepsilon}^{e,trial}_{n+1} + \langle\ \Delta\lambda + c\ f(\boldsymbol{\sigma}_{n+1},\boldsymbol{q}_{n+1})\ \rangle\ \boldsymbol{m}_\sigma(\boldsymbol{\sigma}_{n+1},\boldsymbol{q}_{n+1}) = 0\ ,\\ -\hat{\boldsymbol{\alpha}}(\boldsymbol{\sigma}_{n+1},\boldsymbol{q}_{n+1}) + \boldsymbol{\alpha}^{trial}_{n+1} + \langle\ \Delta\lambda + c\ f(\boldsymbol{\sigma}_{n+1},\boldsymbol{q}_{n+1})\ \rangle\ \boldsymbol{m}_q(\boldsymbol{\sigma}_{n+1},\boldsymbol{q}_{n+1}) = 0\ ,\\ \langle\ \Delta\lambda + c\ f(\boldsymbol{\sigma}_{n+1},\boldsymbol{q}_{n+1})\ \rangle - \Delta\lambda = 0\ , \end{aligned}\right\} \tag{5.11}$$

for the elastic relations $\hat{\boldsymbol{\varepsilon}}^e(\boldsymbol{\sigma},\boldsymbol{q})$ and $\hat{\boldsymbol{\alpha}}(\boldsymbol{\sigma},\boldsymbol{q})$.

2. The above considerations are based on the penalty regularization functions $g(x) = h'(x) = \langle\ x\ \rangle$ of a linear viscoplastic model, with both functions, $g(x)$ and $h(x)$, vanishing for $x \leq 0$. To define the augmented Lagrangian in terms of general penalty functions, we consider the even extension around $x = 0$ of the function $h(x)$ in $x \geq 0$ with its derivative corresponding to the odd extension of the function $g(x)$ in $x \geq 0$, that is, we introduce the functions

$$\widehat{h}(x) := h(|x|) \quad \text{and} \quad \widehat{g}(x) := \widehat{h}'(x) = \text{sign}(x)\ g(|x|)\ , \tag{5.12}$$

for the absolute value $|x|$ and sign function $\text{sign}(x)$. We observe that both $\widehat{h}(x)$ and $\widehat{g}(x)$ are continuous functions (since $h(0) = 0$ and $g(0) = 0$). With these definitions, we can introduce the general augmented Lagrangian

$$\mathcal{L}_c(\boldsymbol{\sigma},\boldsymbol{q},\bar{\lambda}) = \chi(\boldsymbol{\sigma},\boldsymbol{q}) - \boldsymbol{\varepsilon}^{e,trial}_{n+1}\cdot\boldsymbol{\sigma} + \boldsymbol{\alpha}^{trial}_{n+1}\cdot\boldsymbol{q} + c\left[h\Big(\frac{\bar{\lambda}}{c} + f(\boldsymbol{\sigma},\boldsymbol{q})\Big) - \widehat{h}\Big(\frac{\bar{\lambda}}{c}\Big)\right]\ . \tag{5.13}$$

Calculations similar to (5.3)-(5.8) show that Proposition 5.1 holds identically with the generalized augmented Lagrangian, leading to the Euler-Lagrange equations

$$\left.\begin{aligned} \hat{\boldsymbol{\varepsilon}}^e(\boldsymbol{\sigma}_{n+1},\boldsymbol{q}_{n+1}) - \boldsymbol{\varepsilon}^{e,trial}_{n+1} + c\; g\Big(\frac{\Delta\lambda}{c} + f(\boldsymbol{\sigma}_{n+1},\boldsymbol{q}_{n+1})\Big)\; \boldsymbol{m}_\sigma(\boldsymbol{\sigma}_{n+1},\boldsymbol{q}_{n+1}) = 0\;, \\ -\hat{\boldsymbol{\alpha}}(\boldsymbol{\sigma}_{n+1},\boldsymbol{q}_{n+1}) + \boldsymbol{\alpha}^{trial}_{n+1} + c\; g\Big(\frac{\Delta\lambda}{c} + f(\boldsymbol{\sigma}_{n+1},\boldsymbol{q}_{n+1})\Big)\; \boldsymbol{m}_q(\boldsymbol{\sigma}_{n+1},\boldsymbol{q}_{n+1}) = 0\;, \\ g\Big(\frac{\Delta\lambda}{c} + f(\boldsymbol{\sigma}_{n+1},\boldsymbol{q}_{n+1})\Big) - \widehat{g}\Big(\frac{\Delta\lambda}{c}\Big) = 0\;, \end{aligned}\right\} \tag{5.14}$$

in the general form (5.11), with the plastic multiplier given by

$$\Delta\gamma = c\; g\Big(\frac{\Delta\lambda}{c}\Big) \geq 0 \tag{5.15}$$

in this case. Even though the same solution is then obtained (with $f(\sigma_{n+1},\boldsymbol{q}_{n+1}) = 0$, in particular), the consideration of the general augmented Lagrangian (5.13) allows to obtain a general viscoplastic problem as a particular case; see Remark 5.1.2 below. In general, if the rate independent case is the only problem of interest, the choice of a linear viscoplastic regularization given in (5.1) is to be preferred. As shown in Part II in this work, this choice assures the lack of singularities of the Jacobian associated with the three-field system of equations (5.11), as needed when employing a Newton scheme for its solution. □

5.2. Augmented extensions of the dual formulations

The dual variational problem (3.20) can also be extended to an augmented form through the consideration of the dual function

$$\boxed{\phi_c(\bar{\lambda}) = \min_{\{\boldsymbol{\sigma},\boldsymbol{q}\}} \mathcal{L}_c(\boldsymbol{\sigma},\boldsymbol{q},\bar{\lambda})\;,} \tag{5.16}$$

for the augmented Lagrangian $\mathcal{L}_c$ in (5.1), building in the process the dual problem to (5.9). Note that, in contrast with the original dual function (3.19) involving the constraint $\bar{\gamma} \geq 0$, we do not need to impose a similar condition on $\bar{\lambda}$ in (5.16).

A calculation similar to (3.27) leads to the relation

$$\frac{d\phi_c}{d\bar{\lambda}}(\bar{\lambda}) = \frac{1}{c}\Big[\langle \bar{\lambda} + c\; \bar{f}_c(\bar{\lambda})\rangle - \bar{\lambda}\Big] = \max\left\{\bar{f}_c(\bar{\lambda}), -\frac{\bar{\lambda}}{c}\right\}\;, \tag{5.17}$$

where we have introduced the function

$$\bar{f}_c(\bar{\lambda}) := f(\boldsymbol{\Sigma}_c(\bar{\lambda}))\;, \tag{5.18}$$

for the solution $\boldsymbol{\Sigma}_c(\bar{\lambda}) := \{\boldsymbol{\sigma}_c(\bar{\lambda}), \boldsymbol{q}_c(\bar{\lambda})\}$ of the equation

$$\nabla\chi(\boldsymbol{\Sigma}_c(\bar{\lambda})) - \mathcal{I}^{trial} + \langle\ \bar{\lambda} + c\ f(\boldsymbol{\Sigma}_c(\bar{\lambda}))\ \rangle\ \nabla f(\boldsymbol{\Sigma}_c(\bar{\lambda})) = 0\ , \tag{5.19}$$

corresponding to the Euler-Lagrange equation of the minimization problem (5.16) for a fixed $\bar{\lambda}$. From this last expression, we conclude that

$$\begin{aligned} \bar{\lambda} + c\ \bar{f}_c(\bar{\lambda}) \le 0 \quad &\Longrightarrow \quad \boldsymbol{\Sigma}_c(\bar{\gamma}) = \boldsymbol{\Sigma}_{n+1}^{trial} \quad \text{(since then} \quad \langle\ \bar{\lambda} + c\ \bar{f}_c(\bar{\lambda})\ \rangle = 0 \quad \text{in} \quad (5.19)\text{)} \\ &\Longrightarrow \quad \bar{f}_c(\bar{\lambda}) = f(\boldsymbol{\Sigma}_{n+1}^{trial}) = f_{n+1}^{trial} \\ &\Longrightarrow \quad \bar{\lambda} \le -c\ f_{n+1}^{trial} \end{aligned} \tag{5.20}$$

so we have

$$\bar{f}_c(\bar{\lambda}) > -\frac{\bar{\lambda}}{c} \qquad \text{for} \quad \bar{\lambda} > -c\ f_{n+1}^{trial}\ . \tag{5.21}$$

Furthermore, a solution of (5.19) can be easily obtained as $\boldsymbol{\Sigma}_c(\bar{\lambda}) = \boldsymbol{\Sigma}_{n+1}^{trial}$ for $\bar{\lambda} \le -c\ f_{n+1}^{trial}$, so we conclude that

$$\bar{f}_c(\bar{\lambda}) = f_{n+1}^{trial} \qquad \text{for} \quad \bar{\lambda} \le -c\ f_{n+1}^{trial}\ . \tag{5.22}$$

Combining these results with (5.17), we obtain the expression

$$\frac{d\phi_c}{d\bar{\lambda}}(\bar{\lambda}) = \begin{cases} -\frac{\bar{\lambda}}{c}\ , & \text{for } \bar{\lambda} \le -c\ f_{n+1}^{trial}\ , \\ \bar{f}_c(\bar{\lambda})\ , & \text{for } \bar{\lambda} \ge -c\ f_{n+1}^{trial}\ , \end{cases} \tag{5.23}$$

for the derivative of the augmented dual function.

Following an argument similar to the derivation in (3.25)-(3.26) and (3.32), but based on the equation (5.19), we obtain for $\bar{\lambda} > -c\ f_{n+1}^{trial}$ (or, equivalently, $\bar{\lambda}/c + \bar{f}_c(\bar{\lambda}) > 0$ by (5.20)) the relation

$$\frac{d\bar{f}_c}{d\bar{\lambda}}(\bar{\lambda}) = -\ \nabla f \cdot \boldsymbol{H}^{-1} \nabla f < 0\ , \tag{5.24}$$

since the matrix

$$\boldsymbol{H} := \tilde{\boldsymbol{G}}^{-1} + \langle\ \bar{\lambda} + c\ \bar{f}_c(\bar{\lambda})\ \rangle\ \nabla^2 f + c\ H(\bar{\lambda} + c\ \bar{f}_c(\bar{\lambda}))\ \nabla f \otimes \nabla f\ , \tag{5.25}$$

with the Heaviside function $H(x) = \langle x \rangle / x \ge 0$, is a positive definite matrix, given the positive definiteness properties of the matrices $\tilde{\boldsymbol{G}}$ and $\nabla^2 f$ under Assumptions 1 and 2, and $c > 0$. The symbol $\otimes$ in (5.25) denotes the tensor product of two vectors. We conclude that the function $f_c(\bar{\lambda})$ is monotonically decreasing for $\bar{\lambda} > -c\ f_{n+1}^{trial}$.

We next study the equation

$$\frac{d\phi_c}{d\bar{\lambda}}(\Delta\lambda) = 0\ , \tag{5.26}$$

characterizing the extrema $\Delta\lambda$ of the function $\phi_c(\bar{\lambda})$. For an elastic step, that is, $f_{n+1}^{trial} \leq 0$, we conclude from $(5.23)_1$ that a solution is given by $\Delta\lambda = 0$. Furthermore, from $(5.23)_2$ we have

$$\frac{d\phi_c}{d\bar{\lambda}}(\bar{\lambda}) = \bar{f}_c(\bar{\lambda}) < 0 \qquad \text{for} \quad \bar{\lambda} > -c\, f_{n+1}^{trial} \geq 0\,, \tag{5.27}$$

since then $\bar{f}_c(\bar{\lambda}) < f_c(0) = f_{n+1}^{trial} \leq 0$ by the monotonically decreasing character of $f_c(\bar{\lambda})$. Therefore, the only root of the equation (5.26) is given by

$$\Delta\lambda = 0 \qquad \text{for} \quad f_{n+1}^{trial} \leq 0 \quad \text{(elastic step)}\,, \tag{5.28}$$

implying $\Delta\gamma = 0$ by (5.6), since the solution of (5.19) is then $\boldsymbol{\Sigma}_{n+1} = \boldsymbol{\Sigma}_{n+1}^{trial}$ so $f_{n+1} = f_{n+1}^{trial} \leq 0$. Furthermore, we observe that this unique root $\Delta\lambda = 0$ does correspond to a maximum of the function $\phi_c(\bar{\lambda})$, since $d\phi_c^2/d\bar{\lambda}^2(0) = -1/c$ by (5.23) in this elastic case.

Similarly, the equation (5.26) implies

$$\bar{f}_c(\Delta\lambda) = 0 \qquad \text{for} \quad f_{n+1}^{trial} > 0 \quad \text{(plastic step)}\,, \tag{5.29}$$

corresponding to the imposition of the consistency condition for the final solution value $\Delta\lambda$ in this case. We next note that we cannot have $\bar{f}_c(0) \leq 0$ in this case, since then $\boldsymbol{\Sigma}_c(0) = \boldsymbol{\Sigma}_{n+1}^{trial}$ by (5.19), so $\bar{f}_c(0) = f_{n+1}^{trial} > 0$, a contradiction. Since $\bar{f}_c(\bar{\lambda})$ is strictly monotonically decreasing for $\bar{\lambda} \geq -c\, f_{n+1}^{trial}$ (with $-c\, f_{n+1}^{trial} \leq 0$ for this plastic case), we conclude that the root $\Delta\lambda$ is strictly positive and unique. Furthermore, the second derivative of the function $\phi_c(\bar{\lambda})$ at this solution $\Delta\lambda$ reads in this case, after a straightforward calculation,

$$\frac{d^2\phi_c}{d\bar{\lambda}^2}(\Delta\lambda) = -\nabla f \cdot \boldsymbol{H}^{-1} \nabla f < 0\,, \tag{5.30}$$

assuring once more that $\Delta\lambda$ does correspond to a maximum of the function $\phi_c(\bar{\lambda})$.

The above results are summarized in the following proposition, the augmented counterpart of Proposition 3.3.

Proposition 5.2 *Under Assumptions 1 and 2, the plastic multiplier $\Delta\gamma$ in the closest-point projection approximation defined by the equations (2.27) with (2.21) and (2.22) can be characterized as*

$$\Delta\gamma = \langle\ \Delta\lambda + c\ \bar{f}_c(\Delta\lambda)\ \rangle\,, \tag{5.31}$$

(so $\Delta\gamma > 0$ if $\Delta\lambda > 0$, and $\Delta\gamma = 0$ if $\Delta\lambda \leq 0$) for the unique non-negative root $\Delta\lambda$ of the equation

$$\bar{f}_c(\Delta\lambda) = 0\,, \quad \textit{if} \quad f_{n+1}^{trial} > 0 \quad (\Rightarrow\ \Delta\lambda > 0\,, \quad \textit{so} \quad \Delta\gamma = \Delta\lambda > 0)\,, \tag{5.32}$$

or simply

$$\Delta\lambda = 0\,, \qquad \textit{if} \quad f_{n+1}^{trial} \leq 0 \quad (\Rightarrow\ \Delta\gamma = 0)\,, \tag{5.33}$$

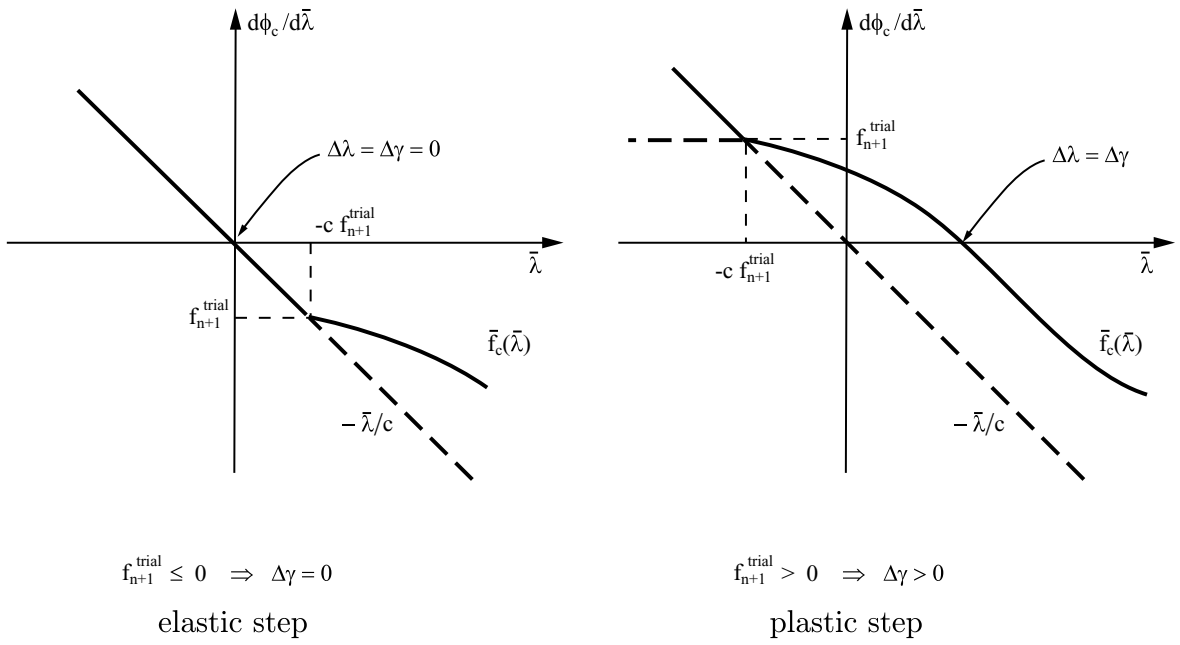

$f_{n+1}^{trial} \leq 0 \;\Rightarrow\; \Delta\gamma = 0$ elastic step

$f_{n+1}^{trial} > 0 \;\Rightarrow\; \Delta\gamma > 0$ plastic step

FIGURE 5.1. Sketch of the function $d\phi_c/d\bar{\lambda}$ for $c > 0$ and the augmented Lagrangian formulation based on a linear viscoplastic regularization. Note that $d\phi_c/d\bar{\lambda}$ is monotonically decreasing and coincides with $\bar{f}_c(\bar{\lambda})$ for $\bar{\lambda} \geq -c\, f_{n+1}^{trial}$ in this case. Furthermore, the unique root is such that $\Delta\lambda = \Delta\gamma$ in this case too.

for the function $\bar{f}_c(\bar{\lambda}) = f(\boldsymbol{\sigma}_c(\bar{\lambda}), \boldsymbol{q}_c(\bar{\lambda}))$*, with* $\{\boldsymbol{\sigma}_c(\bar{\lambda}), \boldsymbol{q}_c(\bar{\lambda})\}$ *corresponding to the argument of the unconstrained minimization problem*

$$\min_{\{\boldsymbol{\sigma},\boldsymbol{q}\}} \left\{ \chi(\boldsymbol{\sigma},\boldsymbol{q}) - \boldsymbol{\varepsilon}_{n+1}^{e,trial} \cdot \boldsymbol{\sigma} + \boldsymbol{\alpha}_{n+1}^{trial} \cdot \boldsymbol{q} + \frac{c}{2} \left[\langle\, \frac{\bar{\lambda}}{c} + f(\boldsymbol{\sigma},\boldsymbol{q}) \,\rangle^2 - \left(\frac{\bar{\lambda}}{c}\right)^2 \right] \right\}, \tag{5.34}$$

for $c > 0$*. The other components of the solution are then simply obtained as* $\{\boldsymbol{\sigma}_{n+1},\, \boldsymbol{q}_{n+1}\} = \{\boldsymbol{\sigma}_c(\Delta\lambda),\, \boldsymbol{q}_c(\Delta\lambda)\}$.

The sketch depicted in Figure 5.1 shows the function $d\phi_c/d\bar{\lambda}$. Since

$$\frac{d^2\phi_c}{d\bar{\lambda}^2}(\bar{\lambda}) = \begin{cases} -\frac{1}{c} < 0 & \text{for } \bar{\lambda} < -c\, f_{n+1}^{trial}\,, \\ -\nabla f \cdot \boldsymbol{H}^{-1} \nabla f < 0 & \text{for } \bar{\lambda} > -c\, f_{n+1}^{trial}\,, \end{cases} \tag{5.35}$$

with all the quantities evaluated at $\boldsymbol{\Sigma}_c(\bar{\lambda})$, we conclude that the augmented dual function $\phi_c(\bar{\lambda})$ is, in fact, a concave function. The equation (5.23) shows the direct relation of the derivative $d\phi_c/d\bar{\lambda}$ with the consistency function $\bar{f}_c(\bar{\lambda})$, a monotonically decreasing function by (5.24) and on the right side of the line $-\bar{\lambda}/c$ by (5.21). The lack of any constraints in the statements of Proposition 5.2 is to be noted. This unconstrained character of the

final formulation is reflected in Figure 5.1, showing the function $d\phi_c/d\bar{\lambda}$ defined for all $\bar{\lambda}$. Figure 5.1 is to be compared with Figure 4.2 for the rate-independent case $\widehat{\eta} = 0$. We can observe how the limit $c \to 0$ leads to the original constrained formulation in Proposition 3.3, with the function $\bar{f}(\bar{\gamma})$ restricted to the case $\bar{\gamma} \geq 0$ only, after identifying $\bar{\lambda}$ with $\bar{\gamma}$ in this limit.

Remarks 5.2.

1. As occurred in the cases considered in the previous sections, the treatment of the equations developed in this section based on the variational structure can be considered in a more general setting not involving the convexity and associativity Assumptions 1 and 2. In this case, the equations (5.32) and (5.33) apply with the function $\bar{f}_c(\bar{\lambda}) = f(\boldsymbol{\sigma}_c(\bar{\lambda}), \boldsymbol{q}_c(\bar{\lambda}))$ defined with the values $\{\boldsymbol{\sigma}_c(\bar{\lambda}), \boldsymbol{q}_c(\bar{\lambda})\}$ given by the augmented equations

$$\left.\begin{aligned} &\hat{\boldsymbol{\varepsilon}}^e(\boldsymbol{\sigma}_c(\bar{\lambda}), \boldsymbol{q}_c(\bar{\lambda})) - \boldsymbol{\varepsilon}^{e,trial}_{n+1} + \langle\ \bar{\lambda} + c\ f(\boldsymbol{\sigma}_c(\bar{\lambda}), \boldsymbol{q}_c(\bar{\lambda}))\ \rangle\ \boldsymbol{m}_\sigma(\boldsymbol{\sigma}_c(\bar{\lambda}), \boldsymbol{q}_c(\bar{\lambda})) = 0\ , \\ &-\hat{\boldsymbol{\alpha}}(\boldsymbol{\sigma}_c(\bar{\lambda}), \boldsymbol{q}_c(\bar{\lambda})) + \boldsymbol{\alpha}^{trial}_{n+1} + \langle\ \bar{\lambda} + c\ f(\boldsymbol{\sigma}_c(\bar{\lambda}), \boldsymbol{q}_c(\bar{\lambda}))\ \rangle\ \boldsymbol{m}_q(\boldsymbol{\sigma}_c(\bar{\lambda}), \boldsymbol{q}_c(\bar{\lambda})) = 0\ , \end{aligned}\right\} \tag{5.36}$$

for a fixed value $\bar{\lambda}$.

2. We note the relation of the augmented formulations developed in this and the previous section for the rate-independent problem with a regularized viscoplastic problem. We simply observe that the value $\bar{\lambda} = 0$ reduces the original augmented Lagrangian (5.1) to the viscoplastic functional in in (4.3) for the linear viscoplastic case, if the penalty parameter c is taken to be $c = 1/\widehat{\eta}$, for the exact viscous parameter $\widehat{\eta}$. The case of a generic viscoplastic function $g(\cdot)$ is obtained through the consideration of the general augmented Lagrangian formulation considered in Remark 5.2.2; all the developments leading to Proposition 5.2 extend to this case. Therefore, the augmented formulation summarized in Proposition 5.2 for the rate-independent case simplifies considerably for the viscoplastic problem, since in this case $\Delta\lambda = 0$ gives the solution directly, without imposing the consistency relation (5.32). The plastic multiplier is then given by the general relation (5.6) since $f_{n+1} \neq 0$ in this case, that is, for a general viscoplastic function

$$\Delta\gamma = c\ g\Big(f(\boldsymbol{\sigma}_{n+1}, \boldsymbol{q}_{n+1})\Big) \qquad \text{for} \quad c = \frac{1}{\widehat{\eta}}\ , \tag{5.37}$$

where $\{\boldsymbol{\sigma}_{n+1}, \boldsymbol{q}_{n+1}\} = \{\boldsymbol{\sigma}_c(0), \boldsymbol{q}_c(0)\}$. As developed in Part II of this work, the numerical algorithms based on the augmented formulation summarized in Proposition 5.2 (or equations (5.36) in general) will involve the search of the root of the consistency equation (5.32), usually starting with the initial trial value $\Delta\lambda = 0$. In the viscoplastic problem, this first iteration will directly provide the final solution. □

6. Concluding Remarks

We have presented in this paper the complete characterization of the variational structure behind the discrete equations defining the closest-point projection approximation in elastoplasticity under the proper convexity assumptions. The results presented herein apply to the infinitesimal range as well as the finite deformation problem in isotropic multiplicative plasticity. Primal and dual variational principles have been investigated for both the constrained rate-independent problem and its Perzyna viscoplastic regularization. The primal principles involve only the stress and stress-like hardening internal variables, with the corresponding Euler-Lagrange equations defining directly the original equations of the closest-point projection approximation. The dual principles presented herein allow the explicit introduction of the plastic multiplier in the variational formulation, leading to a very appropriate framework for the formulation of iterative numerical algorithms that preserve the resulting structure characteristic of the continuum problem. Furthermore, we have explored the formulation of augmented Lagrangian formulation that allow the regularization of the constrained principles in the rate-independent problem while still leading to the solution of the original constrained equations.

The developments presented in this first part of this work identifies clearly the framework for the formulation of efficient numerical algorithms for the solution of the equations of the closest-point projection approximation. The formulation of globally convergent algorithms, in the sense that their convergence is assured for arbitrary initial trial states, while being efficient in computational cost (e.g. exhibiting a quadratic rate of convergence) is our main goal. We undertake this task in Part II of this work.

Acknowledgments: Financial support for this research has been provided by the ONR under contract no. N00014-96-1-0818 and the NSF under contract no. CMS-9703000 with UC Berkeley. A. Perez-Foguet was supported by the Generalitat de Catalunya under grant no. 1998 BEAI200042, and the Commission for Cultural, Educational and Scientific Exchange between the USA and Spain under contract no. 99258 (1999 program), during his stay at UC Berkeley. All this support is gratefully acknowledged.

References

Abbo, A.J. & Sloan, S.W. [1996], "An automatic load stepping algorithm with error control", *Int. J. Num. Meth. Engr.* **39**, 1737-1759.

Anzellotti, G. & Giaquinta, M. [1982], "On the Existence of the Fields of Stresses and Displacements for an Elasto-Perfectly Plastic Body in Static Equilibrium," *Journal of Mathématiques Pures et Appliquée,* **61**, 219-244.

Bertsekas, D.P. [1982] *Constrained Optimization and Lagrange Multiplier Methods,* Athena Scientific, Belmont (reprint of 1996).

Bićanić, N. & Pearce, C.J. [1996], "Computational aspects of a softening plasticity model for plain concrete", *Mechanics of Cohesive and Frictional Materials* **1**, 75-94.

Dutko, M.; Péric, D. & Owen, D.R.J. [1993] "Universal Anisotropic Yield Criterion Based on Superquadratic Functional Representation: Part I. Algorithmic Issues and Accuracy Analysis," *Comp. Meth. Appl. Mech. Engr.,* **109**, 73-93.

Duvaut, G. & Lions, J.L. [1976] *Inequalities in Mechanics and Physics,* Springer-Verlag, Berlin.

Ekeland, I. & Temam, R. [1976] *Convex Analysis and Variational Problems,* North Holland, Amsterdam.

Han, W. & Reddy, B.D. [1999] *Plasticity: Mathematical Theory and Numerical Analysis,* Springer, New York.

Johnson, C. [1976], "Existence Theorems for Plasticity Problems," *Journal de Mathématiques Pures et Appliquée,* **55**, 431-444.

Johnson, C. [1978], "On Plasticity with Hardening," *Journal of Mathematical Analysis and Applications,* **62**, 325-336.

Koiter, W.T. [1960] "General Theorems for Elastic-Plastic Solids," in *Progress in Solid Mechanics,* **6**, 167-221, ed. by I.N. Sneddon and R.Hill, North-Holland, Amsterdam.

Luenberger, D.G. [1989] *Linear and Nonlinear Programming,* Addison-Wesley, Reading.

Matthies, H. [1979], "Existence Theorems in Thermo-plasticity," *Journal de Mecannique* **18**, 695-712.

Matthies, H., Strang G. & Christiansen, E. [1979], "The Saddle Point of a Differential Program," in *Energy Methods in Finite Element Analysis,* ed. by Glowinski, Rodin & Zienkiewicz, J. Wiley & Sons, London, 309-318.

Moreau, J.J. [1976], "Application of Convex Analysis to the Treatment of Elastoplastic Systems," in *Lecture Notes in Mathematics,* ed. P. Germain and B. Nayroles, vol. 503, 56-89.

Moreau, J.J. [1977], "Evolution Problem Associated with a Moving Convex Set in a Hilbert Space," *J. Diff. Eq.* **26**, 347-374.

Ortiz, M. & Simo, J.C. [1986], "Analysis of a New Class of Integration Algorithms for Elastoplastic Constitutive Equations", *Int. J. Num. Meth. Engr.,* **21**, 353-366.

Owen, D.R.J. & Hinton, E. [1980] *Finite Elements in Plasticity ,* Pineridge Press, Swansea.

Papapadopulos, P. & Taylor, R.L. [1994], "On the Application of Multi-Step Integration Methods to Infinitesimal eElastoplasticity", *Int. J. Num. Meth. Engr.,* **37**, 3169-84.

Pérez–Foguet, A., Rodríguez–Ferran, A. & Huerta, A. [1999], "Consistent Tangent Matrices for Substepping Schemes," submitted for publication to *Comp. Meth. Appl. Mech. Engr.*

Perzyna, P. [1966], "Fundamental Problems in Viscoplasticity," in *Advances in Applied Mechanics,* **9**, 244-378.

Perzyna, P. [1971], "Thermodynamic Theory of Viscoplasticity," in *Advances in Applied Mechanics,* **11**, 313-354.

Simo, J.C. [1992], "Algorithms for static and dynamic multiplicative plasticity that preserve the classical return mapping schemes of the infinitesimal theory", *Comp. Meth. Appl. Mech. Engr.,* **98**, 41-104.

Simo, J.C. [1998] "Numerical Analysis of Classical Plasticity", *Handbook for Numerical Analysis, Volume IV,* ed. by P.G. Ciarlet and J.J. Lions, Elseiver, Amsterdam.

Simo, J.C. & Hughes, T.J.R. [1998] *Computational Inelasticity,* Springer, New York.

Simo, J.C. & Ortiz, M. [1985], "A Unified Approach to Finite Deformation Elastoplasticity Based on the Use of Hyperelastic Constitutive Equations", *Comp. Meth. Appl. Mech. Engr.,* **49**, 221-245.

Sloan, S.W. [1987], "Substepping schemes for the numerical integration of elastoplastic stress–strain relations", *Int. J. Num. Meth. Engr.* **24**, 893-911.

de Souza Neto, E.A., Perić, D. & Owen, D.R.J. [1994], "A Model for Elastoplastic Damage at Finite Strains: Algorithmic Issues and Applications", *Engr. Computations* **11**, 257-281.

Suquet, P.M. [1980], "Existence and Regularity of Solutions for Plasticity Problems," in *Variational Methods in the Mechanics of Solids*, ed. by Nemat-Nasser, 304–309.

Suquet, P.M. [1981], "Sur les Équations de la Plasticité: Existence et Regularité des Solutions," *Journal de Mecannique* **20**, 5-39.

Temam, R. [1985], *Mathematical Problems in Plasticity,* Gauthier–Villars, Paris.